Abdel-Rahman for useful discussion. We gratefully acknowledge the technical assistance of Ms T. Ito and Ms S. Shibakawa in the determination of HIV-1 PR inhibitory activity.

REFERENCES

1. Banerjee R, Goldberg DE. In *Antimalarial Chemotherapy*, Rosenthal PJ (ed.). Humana Press: Totawa, NJ, 2001; 43–63.
2. Banerjee R, Liu J, Beatty W, Pelosof L, Klemba M, Goldberg DE. Four plasmepsins are active in the *Plasmodium falciparum* food vacuole, including a protease with an active-site histidine. *Proc. Natl Acad. Sci. USA* 2002; **99**: 990–995.
3. Cooms GH, Goldberg DE, Klemba M, Berry C, Kay J, Mottram JC. Aspartic proteases of *Plasmodium falciparum* and other parasitic protozoa as drug targets. *Trends Parasitol.* 2001; **17**: 532–537.
4. Francis SE, Sullivan DJ Jr, Goldberg DE. Hemoglobin metabolism in the malaria parasite *Plasmodium falciparum*. *Annu. Rev. Microbiol.* 1997; **51**: 97–123.
5. Nezami A, Luque I, Kimura T, Kiso Y, Freire E. Identification and characterization of allophenylnorstatine-based inhibitors of plasmepsin II, an antimalarial target. *Biochemistry* 2002; **41**: 2273–2280.
6. Nezami A, Kimura T, Hidaka K, Kiso A, Liu J, Kiso Y, Goldberg DE, Freire E. High-affinity inhibition of a family of *Plasmodium falciparum* proteases by a designed adaptive inhibitor. *Biochemistry* 2003; **42**: 8459–8464.
7. Francis SE, Gluzman IY, Oksman A, Knickerbocker A, Mueller R, Bryant ML, Sherman DR, Russell DG, Goldberg DE. Molecular characterization and inhibition of a *Plasmodium falciparum* aspartic hemoglobinase. *EMBO J.* 1994; **13**: 306–317.
8. Silva AM, Lee AY, Gulnik SV, Majer P, Collins J, Bhat TN, Collins PJ, Cachau RE, Lurer KE, Gluzman IY, Francis SE, Oksman A, Goldberg DE, Erickson JW. Structure and inhibition of plasmepsin II, a hemoglobin-degrading enzyme from *Plasmodium falciparum*. *Proc. Natl Acad. Sci. USA* 1996; **93**: 10 034–10 039.
9. Moon RP, Tyas L, Certa U, Rupp K, Bur D, Jacquet C, Matile H, Loetscher H, Grueninger-Leitch F, Kay J, Dunn BM, Berry C, Ridley RG. Expression and characterization of plasmepsin I from *Plasmodium falciparum*. *Eur. J. Biochem.* 1997; **244**: 552–560.
10. Carroll CD, Johnson TO, Tao S, Lauri G, Orlowski M, Gluzman IY, Goldberg DE, Dolle RE. Evaluation of a structure-based statine cyclic diamino amide encoded combinatorial library against plasmepsin II and cathepsin D. *Bioorg. Med. Chem. Lett.* 1998; **8**: 3203–3206.
11. Haque TS, Skillman AG, Lee CE, Habashita H, Gluzman IY, Ewing TJA, Goldberg DE, Kuntz ID, Ellman JA. Potent, low-molecular-weight non-peptide inhibitors of malarial aspartyl protease plasmepsin II. *J. Med. Chem.* 1999; **42**: 1428–1440.
12. Ersmark K, Feierberg I, Bjelic S, Hamelink E, Hackett F, Blackman MJ, Hulten J, Samuelsson B, Qvist J, Hallberg A. Potent inhibitors of the *Plasmodium falciparum* enzymes plasmepsin I and II devoid of cathepsin D inhibitory activity. *J. Med. Chem.* 2004; **47**: 110–122.
13. Mimoto T, Imai J, Tanaka S, Hattori N, Kisanuki S, Akaji K, Kiso Y. KNI-102, a novel tripeptide HIV protease inhibitor containing allophenylnorstatine as a transition-state mimic. *Chem. Pharm. Bull.* 1991; **39**: 3088–3090.
14. Kiso Y, Matsumoto H, Mizumoto S, Kimura T, Fujiwara Y, Akaji K. Small dipeptide-based HIV protease inhibitors containing the hydroxymethylcarbonyl isostere as an ideal transition-state mimic. *Biopolymer* 1999; **51**: 59–68.
15. Kiso Y, Yamaguchi S, Matsumoto H, Mimoto T, Kato R, Nojima S, Takaku H, Fukazawa T, Kimura T, Akaji K. KNI-577, a potent small-sized HIV protease inhibitor based on the dipeptide containing the hydroxymethylcarbonyl isostere as an ideal transition-state mimic. *Arch. Pharm. Pharm. Med. Chem.* 1998; **331**: 87–89.
16. Matsumoto H, Kimura T, Hamawaki T, Kumagai A, Goto T, Sano K, Hayashi Y, Kiso Y. Design, synthesis, and biological evaluation of anti-HIV double-drug: conjugates of HIV protease inhibitors with a reverse transcriptase inhibitor through spontaneously cleavable linkers. *Bioorg. Med. Chem.* 2001; **9**: 1589–1600.
17. Mimoto T, Kato R, Takaku H, Nojima S, Terasawa K, Misawa S, Fukazawa T, Ueno T, Sato H, Shintani M, Kiso Y, Hayashi H. Structure–activity relationship of small-sized HIV protease inhibitors containing allophenylnorstatine. *J. Med. Chem.* 1999; **42**: 1789–1802.
18. Kiso Y. Design and synthesis of a covalently linked HIV-1 protease dimer analog and peptidomimetic inhibitors. *J. Synth. Org. Chem., Jpn* 1998; **56**: 896–907.
19. Gluzman IY, Francis SE, Oksman A, Smith CE, Duffin KL, Goldberg DE. Order and specificity of the *Plasmodium falciparum* hemoglobin degradation pathway. *J. Clin. Invest.* 1994; **93**: 1602–1608.
20. KNI-10 006 with Apns-Dmt scaffold is highlighted in Editors' choice. *Science* 2003; **301**: 143.

Biol. Chem., Vol. 385, pp. 1035–1039, November 2004 • Copyright © by Walter de Gruyter • Berlin • New York. DOI 10.1515/BC.2004.134

Minireview

Design of inhibitors against HIV, HTLV-I, and *Plasmodium falciparum* aspartic proteases

Hamdy M. Abdel-Rahman[1], Tooru Kimura[1], Koushi Hidaka[1], Aiko Kiso[1], Azin Nezami[2], Ernesto Freire[2], Yoshio Hayashi[1] and Yoshiaki Kiso[1,*]

[1] Department of Medicinal Chemistry, Center for Frontier Research in Medicinal Science, Kyoto Pharmaceutical University, Yamashina-ku, Kyoto 607-8412, Japan
[2] Department of Biology, The Johns Hopkins University, Baltimore, MD 21218, USA

* Corresponding author
e-mail: kiso@mb.kyoto-phu.ac.jp

Abstract

Aspartic proteases have emerged as targets for substrate-based inhibitor design due to their vital roles in the life cycles of the organisms that cause AIDS, malaria, leukemia, and other infectious diseases. Based on the concept of mimicking the substrate transition-state, we designed and synthesized a novel class of aspartic protease inhibitors containing the hydroxymethylcarbonyl (HMC) isostere. An unnatural amino acid, allophenylnorstatine [Apns; (2*S*,3*S*)-3-amino-2-hydroxy-4-phenylbutyric acid], was incorporated at the P1 site in a series of peptidomimetic compounds that mimic the natural substrates of the HIV, HTLV-I, and malarial aspartic proteases. From extensive structure-activity relationship studies, we were able to identify a series of highly potent peptidomimetic inhibitors of HIV protease. One highly potent inhibitor of the malarial aspartic protease (plasmepsin II) was identified. Finally, a promising lead compound against the HTLV-I protease was identified.

Keywords: AIDS; allophenylnorstatine; antiviral activity; HTLV-I; malaria; protease inhibitors.

Introduction

Aspartic proteases have become important targets of drug development for the treatment of many diseases due to the vital roles they play in the life cycles of many infectious organisms. The proposed mechanism of substrate cleavage by aspartic proteases (Figure 1) shows the formation of a transition state during amide hydrolysis. In designing aspartic protease inhibitors, we have followed the transition-state peptidomimetic principle, i.e., synthesis of a peptide substrate analog that contains a non-hydrolyzable transition-state isostere in place of the normal hydrolyzable P1–P1′ amide bond. This strategy has been utilized to produce structurally diverse and potent HIV protease inhibitors with different transition-state mimetics; indeed, several HIV protease inhibitors have already been approved for clinical treatment of AIDS patients (Kiso, 1996).

In our laboratory, we have successfully designed and synthesized a novel class of peptidomimetic aspartic protease inhibitors containing allophenylnorstatine [Apns; (2*S*,3*S*)-3-amino-2-hydroxy-4-phenylbutyric acid] with a hydroxymethylcarbonyl (HMC) isostere as therapeutic agents for a variety of diseases, such as AIDS, malaria, and leukemia (Kiso et al., 1999; Hamada and Kiso, 2003). Here, we briefly report our latest findings in this field.

HIV protease inhibitors

According to the United Nations program on HIV/AIDS (UNAIDS, 2003) data, the HIV virus is still spreading at an alarming rate; in 2003, approximately 5 million people contracted HIV, and many of these new cases were in sub-Saharan Africa and Southeast Asia. The high infection rate and the appearance of strains that are resistant to approved drugs have made finding novel drug candidates for AIDS treatment of the most challenging problems in medicinal chemistry. Since inhibition of the HIV-encoded protease results in the production of immature and non-infectious virions, intensive research has been devoted to the development of potent HIV protease inhibitors. This strategy has been validated by the approval of several HIV protease inhibitors for clinical use.

To design HIV protease inhibitors, we focused on the Phe-Pro scissile site of HIV protease substrates as the basis for the development of selective HIV protease inhibitors, because HIV protease can recognize Phe-Pro and Tyr-Pro sequences as cleavage sites (Table 1), while mammalian aspartic proteases cannot recognize these sites. Over the course of the last decade, we have reported a series of highly potent peptidomimetic HIV protease inhibitors containing Apns with a HMC isostere. Among these inhibitors, the tripeptide KNI-272 (Figure 2) showed extremely potent HIV protease inhibitory activity (K_i=5.5 pM), high antiviral activity against a wide spectrum of HIV strains, and low cytotoxicity (TC_{50}>80 μM). Furthermore, KNI-272 exhibited excellent enzyme selectivity, with practically no inhibition of other aspartic proteases, such as human plasma renin (IC_{50}>100 000 nM). NMR, X-ray crystallography, and molecular modeling studies have demonstrated that the HMC group in KNI-272 is able to interact excellently with the aspartic-acid carboxyl groups of the HIV-1 protease active site. The hydroxyl group in HMC forms a hydrogen bond to the

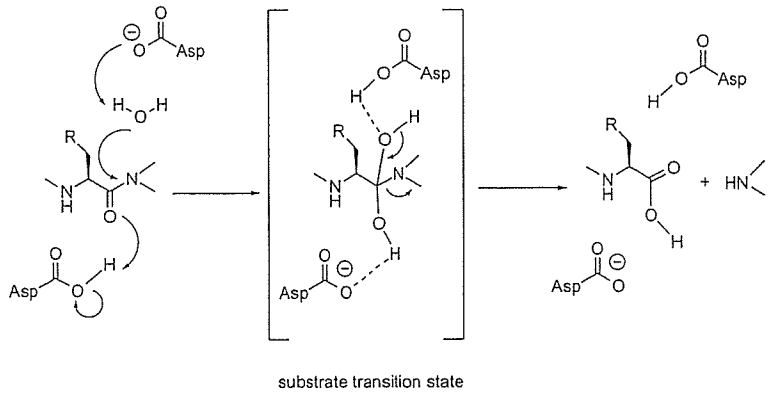

Figure 1 Mechanism of peptide bond hydrolysis by aspartic proteases.

oxygen of Asp125 and the carbonyl oxygen forms a hydrogen bond to the protonated oxygen of Asp25 in essentially the same manner as the transition state of the substrate cleavage (Kiso et al., 1999; Abdel-Rahman et al., 2002).

Further structure-activity relationship (SAR) studies considering the subtle balance of lipophilicity-hydrophilicity and molecular size reduction (Mimoto et al., 1999) resulted in the generation of the conformationally constrained dipeptides KNI-727 and KNI-764 (Figure 2). While both compounds showed potent inhibitory activity against HIV protease, there is a large difference in antiviral activity. The EC_{50} value of KNI-727 was 1.0 μM against wild-type viruses, while that of KNI-764 was 82 nM. Furthermore, KNI-764 completely suppressed all HIV-1 and HIV-2 strains, as well as clinical HIV-1 variants that were highly resistant to all currently available protease inhibitors (Yoshimura et al., 1999).

Structural and thermodynamic information on KNI-764 showed that the better flexibility and adaptability of this inhibitor to the mutated HIV protease are the basis of the mechanism by which this inhibitor can minimize the effects of mutations conferring drug resistance (Velazquez-Campoy et al., 2001; Reiling et al., 2002; Vega et al., 2004). These results suggest that KNI-764 is a promising drug candidate for AIDS treatment, especially against resistant strains.

The structure-metabolism relationships of a series of peptidomimetic HIV protease inhibitors containing substituted Apns have recently been reported (Mimoto et al., 2004). In this study, these compounds not only showed higher stability against P2 phenol glucuronidation than KNI-764, but also showed more potent antiviral activity against both wild-type and multi-drug-resistant HIV-1.

Another important factor in the discovery of HIV protease inhibitors is their antiviral activity in the presence of human serum, as many potent HIV protease inhibitors show reduced antiviral activity in the presence of human serum. For this purpose, a SAR study of Apns-containing dipeptides was carried out, which led to the identification of KNI-1689 (Figure 2). The EC_{50} value of KNI-1689 was 10 nM against wild-type viruses in the absence of human serum, and the potency of this inhibitor was maintained in the presence of 50% human serum, with an EC_{50} value of 82 nM under these conditions (Kimura et al., 2004).

Plasmepsin II inhibitors

Malaria remains a major cause of serious illness and death. As the resistance of the parasite to conventional antimalarial drugs is increasing, the development of novel efficient therapies is urgently needed. Nearly all of the fatal cases of malaria are caused by *Plasmodium falci-*

Table 1 Substrate recognition sites for HIV-1 protease, plasmepsin II, and HTLV-I protease.

Enzyme	Cleavage site	Amino acid sequence						
		P4	P3	P2	P1–P1′	P2′	P3′	P4′
HIV-1 protease	P17/p24	Gln	Arg	Gly	Tyr*Pro	Ile	Val	Gln
	P24/p1	Ala	Arg	Val	Leu*Ala	Glu	Ala	Met
	P1/p9	Ala	Thr	Ile	Met*Met	Gln	Arg	Gly
	P9/p6	Pro	Gly	Asn	Phe*Leu	Gln	Ser	Arg
	TF/PR	Ser	Phe	Asn	Phe*Pro	Gln	Ile	Thr
	PR/RT	Thr	Leu	Asn	Phe*Pro	Ile	Ser	Pro
	RT/RN	Ala	Glu	Thr	Phe*Tyr	Val	Asp	Gly
	RN/IN	Arg	Lys	Ile	Leu*Phe	Leu	Asp	Gly
Plasmepsin II	α 33/34	Glu	Arg	Met	Phe*Leu	Ser	Phe	Pro
	α 108/109	Leu	Leu	Val	Thr*Leu	Ala	Ala	His
	α 136/137	Ser	Thr	Val	Leu*Thr	Ser	Lys	Tyr
	β 32/33	Gly	Arg	Leu	Leu*Val	Val	Tyr	Pro
HTLV-I protease	p19/p24	Pro	Gln	Val	Leu*Pro	Val	Met	His
	p24/p15	Thr	Lys	Val	Leu*Val	Val	Gln	Pro
	TF1/PR	Ala	Ser	Ile	Leu*Pro	Val	Ile	Pro
	PR/p3	Pro	Val	Ile	Leu*Pro	Ile	Gln	Ala
	RT-RH/IN	Val	Leu	Gln	Leu*Ser	Pro	Ala	Phe

TF, transframe protein; PR, protease; RT, reverse transcriptase; RN, ribonuclease H; IN, integrase.

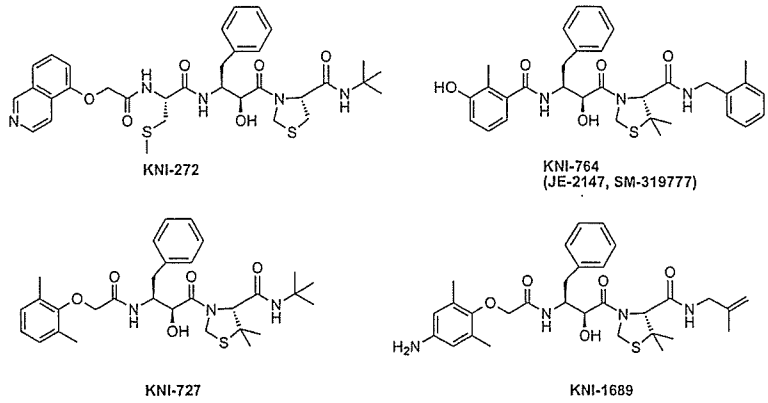

Figure 2 Apns-containing HIV protease inhibitors with the HMC isostere.

parum. This parasite encodes several proteases that are required for its hemoglobin degradation pathway. The acidic food vacuole of *P. falciparum* contains four aspartic proteases, plasmepsin (Plm) I, II, and IV, and a histo-aspartic protease (HAP), which are responsible for hemoglobin degradation (Coombs et al., 2001). These proteases have been recognized as promising targets for therapeutic intervention. Plm II can be easily produced by *E. coli* and the crystal structure of Plm II in complex with pepstatin has been solved. These findings made Plm II the most attractive target for inhibitor design (Boss et al., 2003). As shown in Table 1, the Plm II primary cleavage site is the peptide bond between Phe33 and Leu34 in the hemoglobin α-chain (Hamada and Kiso, 2003). Since the Phe-Leu structure is similar to the Apns-containing scaffold, we hypothesized that our previously prepared HIV-1 inhibitors might also be effective inhibitors of Plm II. Therefore, we evaluated the Plm II inhibitory activity of selected Apns-containing HIV protease inhibitors (Nezami et al., 2002). As predicted, some of these compounds were able to inhibit Plm II potently. KNI-727 (Figure 2) showed potent inhibitory activity, with a K_i value of 70 nM, and 22-fold selectivity in comparison to the highly homologous human enzyme cathepsin D (Cat D). KNI-727 was also effective in killing the malaria parasite, with an EC_{50} value of 10 μM. Further SAR studies (Nezami et al., 2003; Kiso et al., 2004a,b) using KNI-727 as a lead compound resulted in a series of extremely potent inhibitors (Table 2). Among them, KNI-10006 was found to markedly inhibit Plm II, with a K_i value of 0.5 nM.

Table 2 Plasmepsin II and HIV-1 protease inhibition by Apns-based dipeptides.

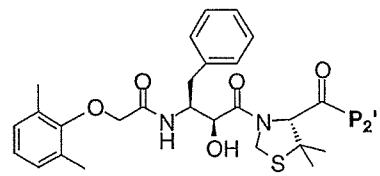

Compound	P2'	K_i (nM)[a]		Inhibition[b] (%)
		Plm II	Cat D	
KNI-727		70	1300	96
KNI-840	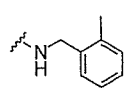	20	80	98
KNI-10026	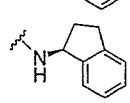	15	105	97
KNI-1269	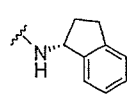	99	-	71
KNI-10006	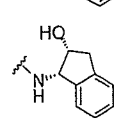	0.5	2	98
KNI-10007	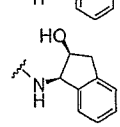	71	806	21

[a]K_i values were determined as described in Nezami et al. (2002).
[b]Percentage HIV PR inhibition in the presence of 50 nM inhibitor.

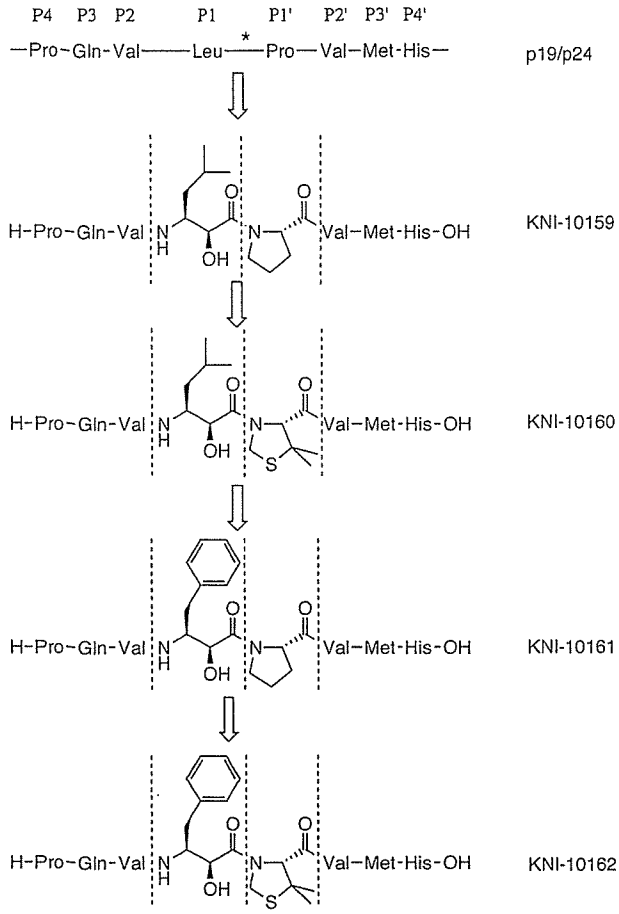

Figure 3 Design of substrate-based HTLV-1 protease inhibitors containing the HMC isostere.

KNI-10006 also showed potent inhibitory activity against Plm I and IV, and HAP.

HTLV-I protease inhibitors

The human T-cell leukemia virus type I (HTLV-I) is a retrovirus that is clinically associated with adult T-cell leukemia (ATL) and myelopathy/tropical spastic paraparesis (HAM/TSP) (Macchi et al., 2003). HTLV-I encodes a virus-specific aspartic protease that is responsible for processing the gag and gag-pro-pol polyproteins, and is required for proliferation of the retrovirus. Therefore, HTLV-I protease is a major target for the development of specific anti-HTLV-I agents (Shuker et al., 2003).

As we had already succeeded in developing HIV protease inhibitors based on the substrate transition-state mimetic concept using the HMC isostere, we thought that this concept might be successfully extended to the development of effective inhibitors of HTLV-I protease. To obtain compounds with potent HTLV-I protease inhibitory activity, we designed and synthesized new substrate-based HTLV-I protease inhibitors mimicking the p19/p24 sequences containing the Leu-Pro cleavage site shown in Table 1. We started the design process (Figure 3) by incorporating the unnatural amino acid allonorstatine [Anst; (2*S*,3*S*)-3-amino-2-hydroxy-5-methylhexanoic acid] with the HMC isostere at the P1 site in an octapeptide, H-Pro-Gln-Val-Leu-Pro-Val-Met-His-OH. From

Table 3 HTLV-I protease inhibition by HMC-based compounds.

Compound	Protease inhibition (%)		
	HTLV-I		HIV[a] 50 nM
	100 μM	5 μM	
KNI-10159	93	43	3
KNI-10160	100	63	37
KNI-10161	94	54	6
KNI-10162	100	66	58
Pepstatin A	-	17	23

For compound structures, see Figure 3.
[a]Percentage HIV PR inhibition in the presence of 50 nM inhibitor.

SAR studies of these compounds (Table 3), we were able to identify KNI-10162, which is an octapeptide similar to the p19/p24 sequence of the enzyme substrate in which the P1 and P1′ amino acid residues are substituted with Apns and dimethylthioproline (Dmt), respectively. KNI-10162 showed 66% inhibition of the rec-HTLV-I protease at 5 μM (Maegawa et al., 2004). In addition, we observed that the recognition of these synthetic inhibitors by the HTLV-I protease was different from that of HIV-1 protease. These results suggest that KNI-10162 may be a useful lead compound for further modification in the development of specific anti-ATL and -HAM drugs (Maegawa et al., 2002).

Conclusion

In summary, we have designed and synthesized a promising class of peptidomimetic Apns-based aspartic protease inhibitors targeting infectious pathogens, such as HIV-1, *P. falciparum*, and HTLV-I. The design of these inhibitors is based on the substrate transition-state mimetic concept. From SAR studies of the HIV-1 protease inhibitors, we were able to identify highly potent compounds that have strong antiviral activity against both wild-type and drug-resistant viruses. KNI-10006 proved to be the most potent inhibitor not only against Plm II, but also against Plm I and IV, and HAP produced by *P. falciparum*. Finally, in a search for inhibitors of HTLV-I protease, KNI-10162 was identified as a promising lead compound for further SAR studies.

Acknowledgments

This research was supported in part by the Frontier Research Program of the Ministry of Education, Science and Culture of Japan, and the Japanese Health Sciences Foundation.

References

Abdel-Rahman, H.M., Al-Karamany, G.S., El-Koussi, N.A., Youssef, A.F., and Kiso, Y. (2002). HIV protease inhibitors: peptidomimetic drugs and future perspectives. Curr. Med. Chem. *9*, 1905–1922.

Boss, C., Richard-Bildstein, S., Weller, T., Fischli, W., Meyerm S., and Binkert, C. (2003). Inhibitors of the *Plasmodium falciparum* parasite aspartic protease plasmepsin II as potential antimalarial agents. Curr. Med. Chem. *10*, 883–907.

Coombs, G.H., Goldberg, D.E., Klemba, M., Berry, C., Kay, J., and Mottram, J. (2001). Aspartic proteases of *Plasmodium falciparum* and other parasitic protozoa as drug targets. Trends Parasitol. *17*, 532–537.

Hamada, Y., and Kiso, Y. (2003). Protease inhibitors: design and new features. Kagaku To Seibutsu *41*, 796–803.

Kimura, T., Hidaka, K., Abdel-Rahman, H.M., Matsumoto, H., Tanaka, Y., Matsui, Y., Hayashi, Y., and Kiso, Y. (2004). Design and synthesis of dipeptide-type HIV-1 protease inhibitors with high antiviral activity. In: Peptide Science 2003, M. Ueki, ed. (Osaka, Japan: The Japanese Peptide Society), pp. 241–244.

Kiso, A., Hidaka, K., Tsuchiya, Y., Kimura, T., Hayashi, Y., Nezami, A., Liu, J., Goldberg, D.E., Freire, E., and Kiso, Y. (2004a). Dipeptide-type inhibitors targeting plasmepsins from *Plasmodium faliciparum*. In: Peptide Science 2003, M. Ueki, ed. (Osaka, Japan: The Japanese Peptide Society), pp. 235–238.

Kiso, A., Hidaka, K., Kimura, T., Hayashi, Y., Nezami, A., Freire, E., and Kiso, Y. (2004b). Search for substrate-based inhibitors fitting the S2′ space of malarial aspartic protease plasmepsin II. J. Peptide Sci., in press.

Kiso, Y. (1996). Design and synthesis of substrate-based peptidomimetic human immunodeficiency virus protease inhibitors containing the hydroxymethylcarbonyl isostere. Biopolymers *40*, 235–244.

Kiso, Y., Matsumoto, H., Mizumoto, S., Kimura, T., Fujiwara, Y., and Akaji, K. (1999). Small dipeptide-based HIV protease inhibitors containing the hydroxymethylcarbonyl isostere as an ideal transition-state mimic. Biopolymers *51*, 59–68.

Macchi, B., Balestrieri, E., and Mastino, A. (2003). Effect of nucleoside-based antiretroviral chemotherapy on human T cell leukemia/lymphotropic virus type 1 (HTLV-I) infection *in vitro*. J. Antimicrob. Chemother. *51*, 1327–1330.

Maegawa, H., Kimura, T., Arii, Y., Matsui, Y., Hayashi, Y., and Kiso, Y. (2002). Identification of peptidomimetic HTLV-I protease inhibitors containing allophenylnorstatine as a transition-state isostere. In: Peptides 2002, E. Benedetti and C. Pedone, eds. (Naples, Italy: Edizioni Ziino), pp. 548–549.

Maegawa, H., Kimura, T., Arii, Y., Matsui, Y., Kasai, S., Hayashi, Y., and Kiso, Y. (2004). Identification of peptidomimetic HTLV-I protease inhibitors containing allophenylnorstatine as the transition-state mimic. Bioorg. Med. Chem. Lett., in press.

Mimoto, T., Kato, R., Takaku, H., Nojima, S., Terashima, K., Misawa, S., Kukazawa, T., Ueno, T., Sato, H., Shintani, M., Kiso, Y., and Hayashi, H. (1999). Structure-activity relationship on small-sized HIV protease inhibitors containing allophenylnorstatine. J. Med. Chem. *42*, 1789–1802.

Mimoto, T., Terashima, K., Nojima, S., Takaku, H., Nakayama, M., Shintani, M., Yamaoka, T., and Hayashi, H. (2004). Structure-activity and structure-metabolism relationships of HIV protease inhibitors containing the 3-hydroxy-2-methylbenzoyl-allophenylnorstatine structure. Bioorg. Med. Chem. *12*, 281–293.

Nezami, A., Laque, I., Kimura, T., Kiso, Y., and Freire, E. (2002). Identification and characterization of allophenylnorstatine-based inhibitors of plasmepsin II, an antimalarial target. Biochemistry *41*, 2273–2280.

Nezami, A., Kimura, T., Hidaka, K., Kiso., A., Liu, J., Kiso, Y., Goldberg, D.E., and Freire, E. (2003). High-affinity inhibition of a family of *Plasmodium falciparum* proteases by a designed adaptive inhibitor. Biochemistry *42*, 8459–8464.

Reiling, K.K., Endres, N.F., Dauber, D.S., Craik, C.S., and Stroud, R.M. (2002). Anisotropic dynamics of the JE-2147-HIV protease complex: drug resistance and thermodynamic binding mode examined in a 1.09 Å structure. Biochemistry *41*, 4582–4594.

Shuker, S.B., Mariani, V.L., Herger, B.E., and Danisson, K.J. (2003). Understanding HTLV-1 protease. Chem. Biol. *10*, 373–380.

UNAIDS and World Health Organization Report (2003). http://www.unaids.org.

Vega, S., Kang, L.-W., Velazquez-Campoy, A., Kiso, Y., Amzel, L.M., and Freire, E. (2004). A structural and thermodynamic escape mechanism from a drug resistant mutation of the HIV-1 protease. Proteins Struct. Funct. Bioinformatics *55*, 594–602.

Velazquez-Campoy, A., Kiso, Y., and Freire, E. (2001). The binding energetics of first and second-generation HIV-1 protease inhibitors: implications for drug design. Arch. Biochem. Biophys. *390*, 169–175.

Yoshimura, K., Kato, R., Yusa, K., Kavlick, M.F., Maroun, V., Nguyen, A., Mimoto, T., Ueno, T., Shintani, M., Falloon, J., et al. (1999). JE-2147: a dipeptide protease inhibitor (PI) that potently inhibits multi-PI-resistant HIV-1. Proc. Natl. Acad. Sci. USA *96*, 8675–8680.

Hamdy M. Abdel-Rahman[a], Nawal A. El-Koussi[a], Gamal S. Alkaramany[a], Adel F. Youssef[a], Yoshiaki Kiso[b]

[a] Pharmaceutical Medicinal Chemistry Department, Faculty of Pharmacy, Assiut University, Assiut 71526, Egypt
[b] Department of Medicinal Chemistry, Kyoto Pharmaceutical University, Kyoto 607-8412, Japan

A Novel Dipeptide-based HIV Protease Inhibitor Containing Allophenylnorstatine

Dipeptide analogues incorporating allophenylnorstatine [Apns; (2S,3S)-3-amino-2-hydroxy-4-phenylbutyric acid] as a transition state mimic at the scissile bond were designed and synthesized in the hope of obtaining a novel KNI series of HIV protease inhibitors. The precursors, N-P_2'-3-(2S,3S)-3-(tert-butyloxycarbonyl)amino-2-hydroxy-4-phenylbutanoyl)-5,5-dimethylthiazolidine-4-carboxamide (N-Boc-Apns-Dmt-P_2') **4a–p** were prepared by deprotection of the synthones N-P_2'-(tert-butyloxycarbonyl)-5,5-dimethylthiazolidine-4-carboxamide (Boc-Dmt-P_2') **2a–p**, then coupling with (2S,3S)3-(*tert*-butyloxycarbonyl)amino-2-hydroxy-4-phenylbutanoic acid (N-Boc-Apns-OH) **3**. The deprotected intermediates **4** were coupled with the activated carboxyl groups of the P_2 ligands to afford the target dipeptides. In this work, we fixed at the P_2 site either a 2,6-dimethylphenoxyacetyl or a 3-hydroxy-2-methylbenzoyl group. Substitutes at the P_2' site were varied to afford the members of the series **7** and **8**. Improved activity of most of the members of series **8** relative to their analogues of series **7** can be partially attributed to the differences in the structures of the P_2 moieties. Positional isomerism in the P_2' moieties significantly affected the activity and polarity of the target.

Keywords: Dipeptide; Antiviral Drugs; HIV Protease Inhibitory Activity; SAR

Received: February 25, 2004; accepted: September 10, 2004 [FP882]
DOI 10.1002/ardp.200400882

Introduction

Inhibition of human immunodeficiency virus (HIV) protease is one of the most important and promising approaches for the treatment of an HIV infection.

The design and development of potent HIV protease inhibitors have generated considerable interest among the AIDS research field and HIV-positive patients. A promising class of HIV protease inhibitors containing allophenylnorstatine (Apns) as a transition state mimic yielded a series of KNI derivatives of highly potent inhibitory properties. In this work, we reported the synthesis of dipeptides with different substituents at the P_2 and P_2' positions with respect to the leads KNI-577 and KNI-901 (see Figure 1) and their protease inhibition activities.

The use of the 2,6-dimethylphenoxyacetyl moiety as P_2 ligand was already reported and provided compounds with potent HIV protease inhibitory activity such as the clinically used drug ABT-378 [1, 2] (Figure 2).

On the other hand, incorporation of the 2,6-dimethylphenoxyacetyl moiety into the KNI series of inhibitors led to the development of highly potent compounds, like the dipeptide KNI-901 [3].

Further challenging of the protease inhibitory activity of the KNI series was practiced by introduction of the

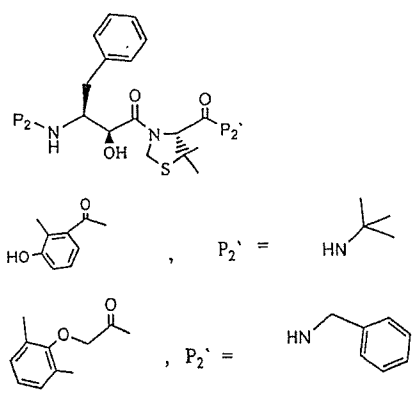

Figure 1. Lead protease inhibition of the KNI series.

Correspondence: Nawal A. El-Koussi, Pharmaceutical Medicinal Chemistry Department, Faculty of Pharmacy, Assiut University, Assiut 71526, Egypt; Phone: +20 88 411297, Fax: +20 88 332776, e-mail: nawal-a@acc.aun.edu.eg

Full Paper

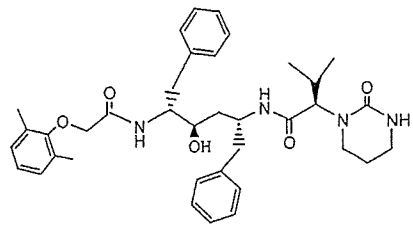

Figure 2. ABT-378 (Lopinavir).

3-hydroxy-2-methylbenzoyl moiety at P_2 sites, which simultaneously provides effective capabilities of hydrophobic and hydrogen bonding interactions with the enzyme relative sites [4].

This approach yielded the highly active KNI-577 [4–7]. The improved activity may be correlated with the combined capabilities of hydrophobic and hydrogen bonding potentialities of their intact moiety.

Guided by the leads KNI-577 and KNI-901, we prepared two series of dipeptide analogues. In one of these series, the P_2 ligand was the 2,6-dimethylphenoxyacetyl moiety as shown by compounds **7** in Table 1. Introduction of the 3-hydroxy-2-methylbenzoyl moiety at the P_2 site provided the second series of dipeptides represented by the compounds **8** in Table 2. In series **7** and **8**, P_2' was changed in the hope to improve protease inhibition potential and enhance polarity. It is clear that the partition coefficient, represented by the Rt value, and solubility are closely related phenomena; therefore, the choice of moieties at P_2' with predominant polar functions was targeted in both series [8, 9].

Results and discussion

Chemistry

The target dipeptide inhibitors were prepared as illustrated in Scheme 1, starting from 5,5-dimethylthiazolidine-3-carboxylic acid (Dmt-OH), which was prepared by cyclization of L-penicillamine with formaldehyde, followed by N-protection by Boc to yield Boc-Dmt-OH **1** according to reported procedures [10]. Coupling of the amino ligands $P_2'NH_2$ with **1** in the presence of 1-hydroxybenzotriazole (HOBt) in DMF [11, 12] or diphenylphosphochloridate (DPPCl), Et_3N and AcOEt [13] afforded the intermediates **2a–p** (Table 3). N-elimination of the Boc moiety and coupling with Boc-Apns-OH **3** by either 1-ethyl-3-(3′-dimethylaminopropyl) carbodiimide (EDC) or benzotriazole-1-yloxytris-(dimethylamino) phosphonium hexafluorophosphate (BOP) in the presence of HOBt in DMF [14] yielded the synthones **4a–p** (Table 4). These intermediates were used as scaffolds for the synthesis of the targets **7** and **8**. 2,6-Dimethylphenoxyacetic acid **5** was activated by EDC, HOBt in DMF or THF and coupled with the deprotected **4a–n** to afford the series **7a–n** (Table 1). In series **8**, 3-acetyl-2-methylbenzoic acid **6** was activated by DPPCl in AcOEt and then coupled with the deprotected synthones **4a–h**, **o** and **p**. Hydrolytic cleavage of the 3-acetyl group by LiOH yielded **8a–h**, **o** and **p** dipeptides in Table 2. The final compounds obtained after crystallization were checked by analytical HPLC; from the resulting data, preparative HPLC was established and carried out. The purity was checked again by analytical HPLC. The fractions were mixed and lyophilized to afford the analytically pure final compounds; yields of the products were determined by reversed-phase HPLC (RP-HPLC). Within each series, the parallelism between Rt of the compounds and the polarity of the P_2' moieties could be easily observed. The effect of the location of the polar groups in the P_2' moieties on the Rt values of the positional isomers **7g, h, i, k, l, m, n** and in **8g, h, o, p** was perceptible. Homogenity of targets **7** and **8** was checked by TLC using two systems of different polarities: chloroform/methanol (10:1) and chloroform/methanol/water (8:3:1).

Structure activity relationship against HIV-1 protease

The effect of variation of the P_2' moieties on HIV-1 protease inhibition of the potent leads KNI-901 and KNI-577 was regarded as the main objective of the present study. The benzylamino group at the P_2' site in KNI-901 was the target modified to afford the dipeptides **7**, whereas the t-butyl group at the P_2' site in KNI-577 was replaced by the same modified benzylamino derivatives to afford almost all members of series **8**.

Three approaches were considered for modification of the benzylamine moiety. First, the assumption that the phenyl ring must be distanced by one atom from the amidic NH represents an essential requisite. Groups of different bulkiness and polarity, with one atom bridging the phenyl ring and the amidic NH, were inserted to replace the α-methylene group in benzylamine. This approach was challenged by the compounds **7a, b, e** and **8a, b, e.** As shown in Table 5, compounds **7b** and **8b** with inserted α-N (CH_3) were the least active ones. On the other hand, the 2-isopropylene bridge significantly improved the activity of **7a** and **8a**, which are still less active than the corresponding leads. Compound **8e** revealed 91.2% inhibition potential, which is higher than the potential of the lead KNI-577. Matching the activities of **7a, e** with their analogues **8a, e** dem-

onstrated a boosting effect of the P_2 moiety in series **8**. Secondly, introduction of a polar substitute at the *o*-, *m*-, or *p*-position on the benzene ring was tried by preparing **7c, d, f, k–n** and **8c, d, f** dipeptides. All these isomers were less active than the leads; however, the derivatives of the **8** series still revealed a

Table 1. Physical data of dipeptide-based HIV protease inhibitors **7**.

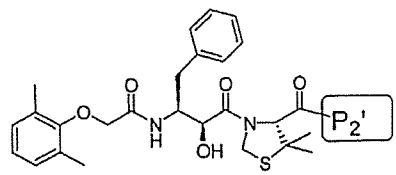

No.	P_2'	mp (°C)	Yield (%)	HPLC[§] Rt (min)	TLC Rf_1[†]	TLC Rf_2[¥]
7a	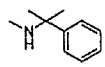	89–90	85	27.44	0.98	0.96
7b	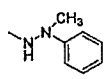	115–117	54.5	24.81	0.81	0.90
7c	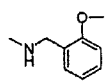	89–91	65	26.37	0.68	0.89
7d	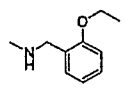	85–88	71	27.12	0.72	0.90
7e[#]	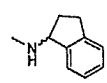	103–105	61	27.28	0.90	0.96
7f	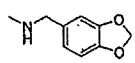	110–113	78	25.08	0.90	0.93
7g	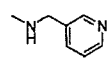	107–108	71	16.92	0.80	0.86
7h	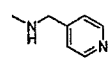	141–143	70	17.34	0.62	0.77
7i	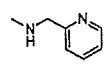	98–100	73	18.10	0.68	0.84
7j	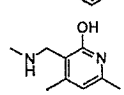	149–151	55	21.10	0.62	0.77
7k	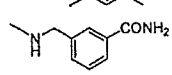	124–126	79	20.38	0.54	0.83
7l	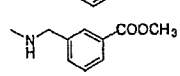	98–100	53	24.70	0.84	0.91
7m	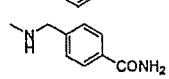	140–142	57	19.81	0.52	0.90
7n	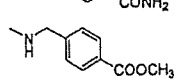	99–100	63	24.38	0.89	0.94

[#] Mixture of diastereomers; [§] 20–80% CH_3CN in 0.1% aqueous TFA over 30 min; [†] $CHCl_3/CH_3OH$ (10:1); [¥] $CHCl_3/CH_3OH/H_2O$ (8:3:1).

Table 2. Physical data of dipeptide-based HIV protease inhibitors **8**.

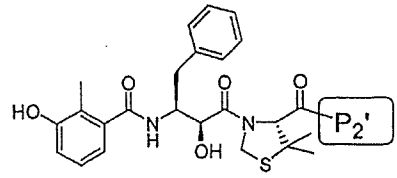

No.	P_2'	mp (°C)	Yield (%)	HPLC[§] Rt (min)	TLC	
					Rf_1[†]	Rf_2[¥]
8a	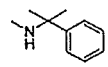	128–130	65.5	20.86	0.69	0.88
8b	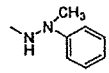	150–152	78	18.08	0.37	0.76
8c	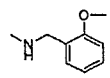	127–129	68	19.45	0.57	0.83
8d	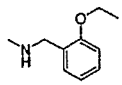	121–123	72	21.10	0.67	0.86
8e[#]	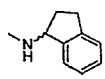	139–141	58	20.42 20.52	0.56	0.76
8f	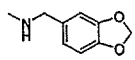	139–140	71	20.24	0.59	0.67
8g	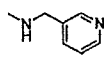	141–143	35.5	11.47	0.58	0.80
8h	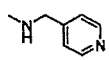	154–156	24	9.94	0.35	0.65
8o	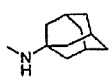	153–155	76	27.15	0.56	0.66
8p	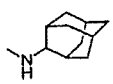	159–161	66	26.64	0.54	0.70

[#], [§], [†] and [¥] as in Table 1.

higher pattern of activity that can only be attributed to the different P_2 moieties. Finally, the benzyl moiety was replaced by the bioisosteric α-, β-, and γ-picolines. This approach yielded the most active derivative **7g**, which is equally active as the lead KNI-901, with an apparently enhanced polarity. Improvement of polarity presumably may advantageously affect its absorption and distribution properties. Furthermore, the presence of a basic pyridine center allows for formation of salts.

The significantly reduced activity of the α-picolinyl derivative **7i** may be attributed to the possible competition for intramolecular hydrogen bond formation between the pyridine N and the amidic NH, which participates in a crucial hydrogen bonding with the water molecule bridging Ala28 and Asp29 in the S_2' site of the enzyme [15]. In the absence of such interaction, higher activity of the β- and γ-picoline **7g** and **7h** was observed. On the other hand, the lowered activity of the alkoxy **7c**, **d**, **8c**, **d** and 4,6-dimethyl-1,2-dihydro-3-

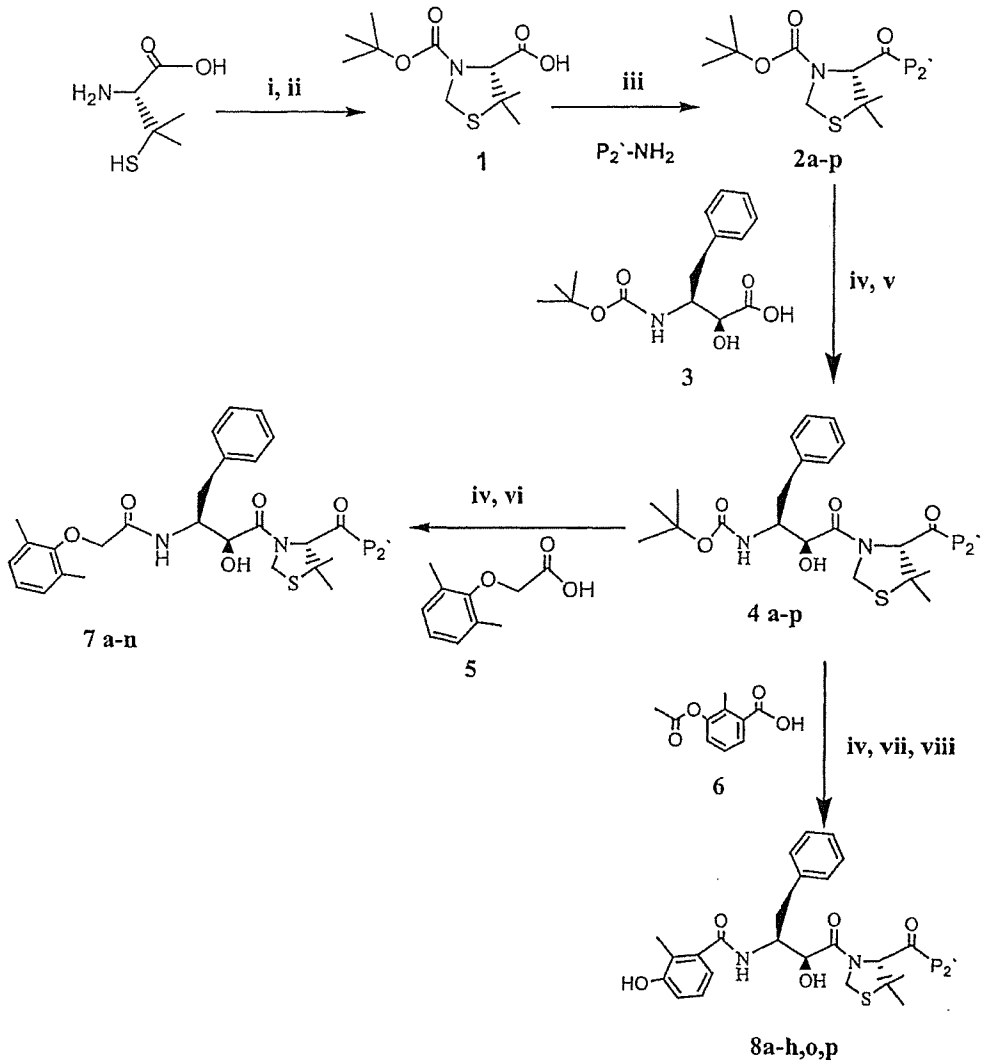

(i) aq 37% HCHO (ii) $(Boc)_2O$ (iii) HOBt in DMF or DPPCl, Et_3N, AcOEt(iv) N HCl/dioxane

(v) EDC, HOBt in DMFor BOP, HOBt in DMF (vi) EDC, HOBt in DMFor THF

(vii) DPPCl in AcOEt, (viii) LIOH

Scheme 1. Synthesis of dipeptides 7 and 8.

picolinyl-2- one **7j** can be equally attributed to possible intramolecular hydrogen bonding between the unshared pair of electrons on the *o*-oxygen and the amidic NH.

Positional isomers of the substituted benzyl amines and of the picolines revealed a significant impact on activity. The β-picolinyl **7g**, and **8g** and the *m*-substituted benzyl derivatives **7k**, **l** on the one hand exerted

Table 3. Physical data of intermediate compounds N-Boc-Dmt-P_2' **2.**

No.	P_2'	mp (°C)	HPLC[§] Rt (min)	No.	P_2'	mp (°C)	HPLC[§] Rt (min)
2a	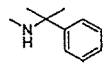	102–104	23.24	**2i**	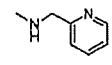	116–119	10.29
2b	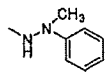	185–188	19.71	**2j**	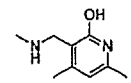	128–130	13.30
2c	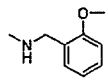	112–113	23.34	**2k**	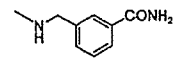	88–89	13.48
2d	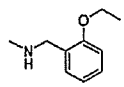	113–114	22.92	**2l**	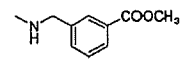	‡	20.14
2e[#]	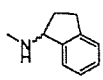	60–62	23.92 24.16	**2m**	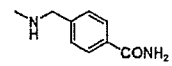	107–109	13.92
2f	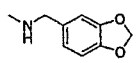	124–126	21.68	**2n**	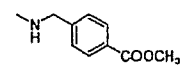	115–116	20.96
2g	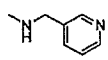	‡	7.68	**2o**	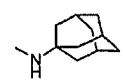	155–156	30.56
2h	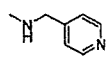	162–164	9.86	**2p**	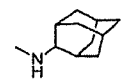	178–179	30.10

[#] Mixture of diastereomers; [§] 20–80% CH_3CN in 0.1% aqueous TFA over 30 min; [‡] not determined, sticky semisolid material.

a relatively higher activity when matched with the γ-picolines **7h**, and **8h** and the *p*-substituted benzyls **7m, n** on the other hand. A common feature of these isomers is the availability of an atom or group on the aromatic ring that carries an unshared pair of electrons. It seems feasible to correlate the observed differences in activity with the unshared pair of electrons that should be suitably oriented at a critical distance from the amidic NH. Deviation from this critical distance might lead to decreased activity. Thus, a location of the unshared pair of electrons separated by three carbons from the amidic NH seems to give the optimum activity, as in **7g**. Shifting of the unshared pair of electrons on N towards α- or γ-positions either gets it involved in intramolecular hydrogen bonding, as in **7i**, or diminishes its supporting role of interaction with the enzyme, as in **7h**. By analogy, the differences in activities of the *m*- and *p*-isomers of benzylcarboxamides **7k** and **7m** and the methyl benzylcarboxylates **7l** and **7n** were found to parallel the distance separating the carbonyl oxygen from the amidic NH.

The tolerance of the S_2' site to accommodate a bulky substituent was challenged by the attachment of 1- or 2- adamantyl groups, which can be regarded as the constrained analogues of the tert-butyl moiety at the P_2' position in the lead KNI-577. The yielded dipeptides **8o** and **8p** were found to be the least active derivatives.

Conclusions

KNI-577 and KNI-901 leads are substrate-based HIV protease inhibitors. The two leads are members of the KNI series containing allophenylnorstatine (Apns) with hydroxymethylcarbonyl isostere as a transition state mimic at the scissile peptide bond.

The activity of the prepared series of P_2-Apns-Dmt-P_2' strongly depends on the simultaneous balance between electronic and steric properties of both the P_2 and P_2' moieties. As shown from Table 5, the ability of interaction of P_2 and P_2' with the relevant enzyme

Table 4. Physical data of intermediate compounds N-Boc-Dmt-P_2' 4.

No.	P_2'	mp (°C)	HPLC§ Rt (min)	No.	P_2'	mp (°C)	HPLC§ Rt (min)
4a	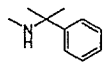	102–106	25.56	**4i**	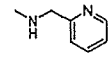	94–98	15.52
4b	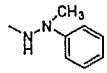	106–109	22.72	**4j**	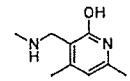	147–150	18.87
4c	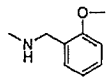	99–102	23.70	**4k**	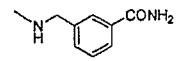	132–135	18.80
4d	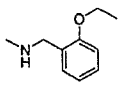	100–103	25.57	**4l**	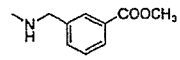	117–120	25.44
4e#	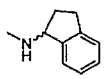	95–98	25.06 25.23	**4m**	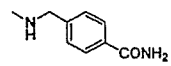	96–99	17.78
4f	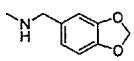	75–78	25.66	**4n**	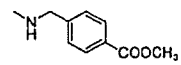	110–112	22.66
4g	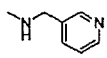	96–100	16.19	**4o**	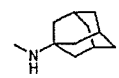	103–106	32.75
4h	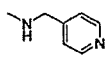	105–109	14.92	**4p**	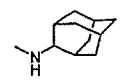	107–109	31.94

and § as in Table 3.

sites S_2 and S_2' would significantly affect the fitting of Apns to the enzyme catalytic site, which reflects the HIV protease inhibitory activity.

Two derivatives were found to be equally or more active than the leads KNI-577 and KNI-901 and present promising candidates for further investigations.

Experimental

Melting points were determined on a micro hot plate of a Yanaco micro melting point apparatus and were uncorrected. The optical rotations were measured on a Horiba model SEPA-300 digital polarimeter. TLC was performed on precoated Merck silica gel 60 F_{254} sheets. Column chromatography was carried out on Merck silica gel 60 (particle size 0.063–0.200 mm).

Analytical RP-HPLC was performed with a Hitachi L-7100 pump and an L-7400 UV detector utilizing YMC Pack ODS-AM AM 302.

Preparative RP-HPLC was performed with a Shimadzu LC-4A liquid chromatograph utilizing a YMC Pack ODS-AM type SH-343-5AM column (250 × 20 mm i.d., S-5 μm, 120 A).

^{1}H NMR spectra were recorded on a JEOL JNM-EX 270 (270 MHz) spectrometer. Chemical shifts are given in (δ ppm) relative to tetramethylsilane (TMS) as an internal standard. 13C NMR spectra were recorded on a JEOL JNM-EX 270 (67.5 MHz) using solvents as internal standard. FAB mass spectra (FAB-MS) and high-resolution FAB-MS (HRFAB-MS) were recorded on a JEOL JMS-SX102 AQQ/MS-HYB10 mass spectrometer using glycerol, thioglycerol or Magic Bullet as internal references. MALDI TOF mass spectra were measured at Voyager-DE™RP Biospectrometry™ Workstation (PerSeptive Biosystems). Commercially available chemicals were purchased from Nacalai tesque, Waku Chemicals or Tokyo Chemical Industries, Japan, and were used without further purification. Commercially non-available chemicals were prepared according to standard methods described in [16] and showed 1H NMR and 13C NMR spectra in accordance with the assigned structures.

(tert-Butyloxycarbonyl)-5,5-dimethylthiazolidine-4-carboxylic acid Boc-Dmt-OH (1) [10]

Yield 81%, mp 124–127°C.

N-P_2'-(tert-Butyloxycarbonyl)-5,5-dimethylthiazolidine-4-carboxamide Boc-Dmt-P_2' (2a–p)

Table 5. HIV protease inhibitory activity of targeted dipeptides P_2-Apns-Dmt-P_2' **7** and **8**.

No.	P_2 = 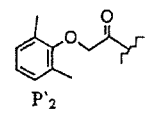	% HIV protease inhibition (50 nM)	No.	P_2 = 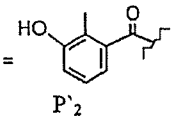	% HIV protease inhibition (50 nM)
7a	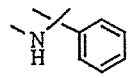	72.5	**8a**	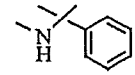	82.2
7b	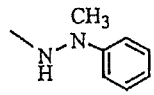	15.3	**8b**	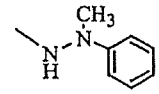	12.9
7c	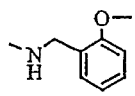	24.0	**8c**	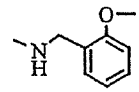	65.8
7d	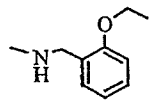	41.7	**8d**	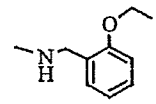	49.7
7e[#]	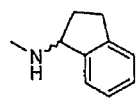	64.5	**8e**[#]	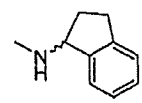	91.2
7f	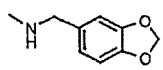	27.6	**8f**	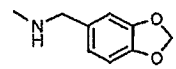	67.6
7g	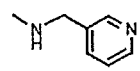	86.8	**8g**	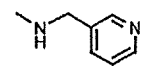	62.6
7h	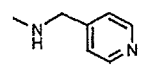	70.7	**8h**	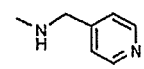	34.5
7i	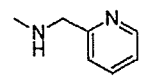	57.8	**8o**	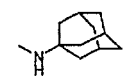	7.1
7j	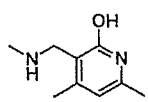	20.9	**8p**	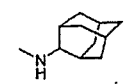	5.5
7k	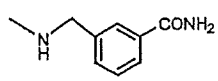	67.7	KNI-577	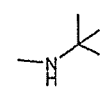	87.6
7l	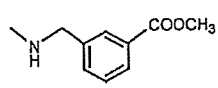	45.0			
7m	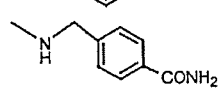	3.3			
7n	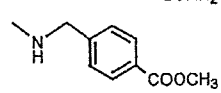	28.6			
KNI-901	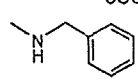	86			

[#] mixture of diasteromers.

Boc-Dmt-OH (1.5 g, 5.74 mmol) was dissolved and stirred in AcOEt (20 mL); Et_3N (0.88 mL, 6.33 mmol) and DPPCl (1.31 mL, 6.33 mmol) were added at 0 °C. The mixture was stirred at room temperature for 1 h, then appropriate amine (6.33 mmol) and Et_3N (0.88 mL, 6.33 mmol) were added. Stirring was continued at room temperature for 6 h. The mixture was washed twice with 10% citric acid, 5% $NaHCO_3$ and brine, dried over anhydrous Na_2SO_4 and filtered. The filtrate was evaporated under reduced pressure, crystallized from *n*-hexane and dried in a dessicator [16, 17].

(2S,3S)3-(tert-Butyloxycarbonyl)amino-2-hydroxy-4-phenylbutanoic acid N-Boc-Apns-OH (3) [18]

Yield 8%, mp147–148 °C.

N-P_2'-3-(2S,3S)-3-(tert-butyloxycarbonyl)amino-2-hydroxy-4-phenylbutanoyl)-5,5-dimethylthiazolidine-4-carboxamide Boc-Apns-Dmt-P_2' (4a–p)

To the appropriate Boc-Dmt-P_2' **2a–p** (0.5 mmol) in 4 N HCl/dioxane solution (2 mL), anisol (108 µL, 1 mmol) was added at 0 °C. This solution was stirred for 2 h at room temperature. The solvent was evaporated *in vacuo*, ether was added, the mixture was centrifuged, and the residue was dissolved in DMF (5 mL). Boc-Apns-OH **3** (134 mg, 0.45 mmol), HOBt.H_2O (76.6 mg, 0.5 mmol), BOP (211 mg, 0.5 mmol) and Et_3N (139 mL, 1 mmol) were added at 0 °C. The mixture was stirred overnight at room temperature. The solvent was then removed under vacuum and the residue was extracted with AcOEt. The organic layer was washed with 10% citric acid, 5% $NaHCO_3$ and brine, dried over anhydrous Na_2SO_4 and filtered. The filtrate was evaporated under reduced pressure. The residue was purified by column chromatography, and the appropriate fractions were pooled and evaporated to yield the coupled peptide (Boc-Apns-Dmt-P_2'), which was dried in a desiccator [16, 17].

2,6-Dimethylphenoxyacetic acid (5)

Compound **5** was synthesized starting from 2,6-dimethyl phenol by alkylation with ethyl-2-bromoacetate, then hydrolysis. Yield 37%, mp138–139 °C.

3-Hydroxy-2-methylbenzoic acid [16]

Yield 86.5%, mp142–144 °C.

3-Acetyloxy-2-methylbenzoic acid (6)

Acetylation of 3-hydroxy-2-methylbenzoic acid yielded 3-acetyloxy-2-methylbenzoic acid **6** (quantitative, mp 147–148 °C).

Synthesis of dipeptides containing 2,6-dimethyl phenoxyacetic acid as P_2 ligand (2,6-dimethylphenoxyacetyl-Apns-Dmt-P_2') (7a–n)

The titled compounds were prepared, starting from N-Boc-Apns-Dmt-P_2' **4a–n** (20.8 mmol) in 4 N HCl/dioxane (40 mL); anisole (4.5 mL, 41.67 mmol) was added at 0 °C. The reaction mixture was stirred for 1 h at room temperature, and the solvent was then removed *in vacuo* at room temperature; ether was added, and the mixture was centrifuged. The formed precipitate was dissolved in DMF (40 mL), and then 2,6-dimethylphenoxyacetic acid **5** (22.85 mmol), HOBt.H_2O (3.5 g, 22.85 mmol), EDC.HCl (4.3 g, 22.43 mmol) and Et_3N (5.78 mL, 41.6 mmol) were added at 0 °C. The reaction mixture was stirred overnight at room temperature, and the solvent was removed under reduced pressure. The residue was extracted with AcOEt. The organic layer was washed with 10% citric acid, 5% $NaHCO_3$ and brine, dried over anhydrous Na_2SO_4, filtered and evaporated. The residue was crystallized from *n*-hexane. Physical data are listed in Table 1.

2,6-Dimethylphenoxyacetyl-Apns-Dmt-NH-cumyl (7a)

$[a]_D^{28}$ −1.60 (c = 0.218, CH_3OH), ^1H NMR (DMSO-d_6) δ: 1.43 (s, 3H), 1.49 (s, 1H), 1.54 (s, 3H), 1.65 (s, 3H), 2.16 (s, 6H), 2.70–2.73 (m, 2H), 3.99–4.05 (d, *J* = 14.51 Hz, 1H), 4.14–4.20 (d, *J* = 13.85 Hz, 1H), 4.28 (bs, 1H), 4.42 (s, 1H), 4.66 (s, 1H), 4.84–4.93 (m, 2H), 6.92–7.02 (m, 3H), 7.15–7.24 (m, 10H), 7.41–7.44 (d, *J* = 7.69 Hz, 1H), 8.24–8.27 (d, *J* = 8.58 Hz, 1H), HRFAB-MS: *m/z* 618.3004 for $[M+H]^+$ (calcd. 618.3002 for $C_{35}H_{44}N_3O_5S$).

2,6-Dimethylphenoxyacetyl-Apns-Dmt-NH-MPH (7b)

$[a]_D^{24.9}$ −11.42 (c = 0.07, CH_3OH), ^1H NMR (DMSO-d_6) δ: 1.49 (s, 3H), 1.58 (s, 3H), 2.16 (s, 6H), 2.76–2.82 (m, 2H), 3.97–4.02 (d, *J* = 13.53 Hz, 1H), 4.15–4.20 (d, *J* = 13.52 Hz, 1H), 4.26–4.48 (m, 3H), 4.97–5.00 (m, 2H), 6.68–6.71 (t, *J* = 7.26 Hz, 1H), 6.81–7.03 (m, 4H), 7.12–7.25 (m, 8H), 8.17–8.20 (d, *J* = 8.91 Hz, 1H), 10.17 (s, 1H), HRFAB-MS: *m/z* 605.2804 for $[M+H]^+$ (calcd. 605.2798 for $C_{33}H_{41}N_4O_5S$).

2,6-Dimethylphenoxyacetyl-Apns-Dmt-NH-(2-OCH_3)Bz (7c)

$[a]_D^{24}$ *− 14.85 (c = 0.202, CH_3OH)*, ^1H NMR (DMSO-d_6) δ: 1.34 (s, 3H), 1.50 (s, 3H), 2.14 (s, 6H), 2.77–2.80 (m, 2H), 3.77 (s, 3H), 3.97–4.02 (d, *J* = 14.19 Hz, 1H), 4.13–4.18 (d, *J* = 14.18 Hz, 1H), 4.25–4.27 (d, J = 5.28 Hz, 2H), 4.37–4.40 (m, 1H), 4.46–4.49 (m, 2H), 4.91–5.00 (m, 2H), 6.79–6.85 (t, *J* = 7.59 Hz, 1H), 6.89–7.01 (m, 2H), 7.15–7.30 (m, 9H), 8.12–8.15 (d, *J* = 8.57 Hz, 1H), 8.27–8.35 (t, *J* = 5.6 Hz, 1H), HRFAB-MS: *m/z* 620.2854 for $[M+H]^+$ (calcd. 620.2794 for $C_{34}H_{42}N_3O_6S$).

2,6-Dimethylphenoxyacetyl-Apns-Dmt-NH-(2-OC_2H_5)Bz (7d)

$[a]_D^{27.3}$ *−9.96 (c = 0.158, CH_3OH)*, ^1H NMR (DMSO-d_6) δ: 1.31–1.35 (m, 6H), 1.51 (s, 3H), 2.14 (s, 6H), 2.77–2.80 (m, 2H), 3.93–4.05 (m, 3H), 4.12–4.18 (m, 1H), 4.26–4.28 (d, *J* = 4.29 Hz, 2H), 4.39 (s, 1H), 4.47–4.50 (m, 2H), 4.92–5.00 (m, 2H), 6.78–6.83 (t, *J* = 6.27 Hz, 1H), 6.90–7.01 (m, 3H), 7.12–7.30 (m, 7H), 8.13–8.15 (d, *J* = 7.91 Hz, 1H), 8.30 (t, *J* = 5.6 Hz, 1H), HRFAB-MS: *m/z* 634.2969 for $[M+H]^+$ (calcd. 634.2951 for $C_{35}H_{44}N_3O_6S$).

2,6-Dimethylphenoxyacetyl-Apns-Dmt-NH-Ind (7e)

$[a]_D^{25}$ +19.86 (c = 0.448, CH_3OH), ^1H NMR (DMSO-d_6) δ: 1.44 (s, 3H), 1.51 (s, 3H), 1.79–1.84 (m, 1H), 2.15 (s, 6H), 2.34–2.40 (m, 1H), 2.81–2.91 (m, 4H), 3.95–4.02 (m, 1H), 4.16–4.22 (m, 1H), 4.39–4.50 (m, 3H), 4.98–4.99 (m, 2H), 5.32–5.35 (m, 1H), 6.90–7.08 (m, 4H), 7.17–7.38 (m, 8H), 8.14–8.17 (d, *J* = 8.24 Hz, 1H), 8.35–8.45 (dd, *J* = 8.24 Hz, 1H), HRFAB-MS: *m/z* 616.2878 for $[M+H]^+$ (calcd. 616.2845 for $C_{35}H_{42}N_3O_5S$), TOF-MS 616.727 for $[M+H]^+$.

2,6-Dimethylphenoxyacetyl-Apns-Dmt-NH-Pip (7f)

$[a]_D^{27}$ −2.00 (c = 0.15, CH_3OH), ^1H NMR (DMSO-d_6) δ: 1.34 (s, 3H), 1.51 (s, 3H), 2.15 (s, 6H), 2.76–2.80 (m, 2H), 3.99–4.02 (m, 1H), 4.14–4.29 (m, 3H), 4.34–4.48 (m, 3H),

4.97 (s, 2H), 5.88–5.92 (m, 2H), 6.77 (s, 2H), 6.85 (s, 1H), 6.95–7.02 (m, 3H), 7.19–7.30 (m, 4H), 8.09–8.13 (d, J = 9.17 Hz, 1H), 8.43–8.48 (t, J = 6.11 Hz, 1H), HRFAB-MS: m/z 634.2583 for $[M+H]^+$ (calcd. 634.2587 for $C_{34}H_{40}N_3O_7S$).

*2,6-Dimethylphenoxyacetyl-Apns-Dmt-NH-3-picolyl (**7g**)*

$[a]_D^{3.8}$ +47.14 (c = 0.28, CH_3OH), ^1H NMR (DMSO-d_6) δ: 1.34 (s, 3H), 1.53 (s, 3H), 2.12 (s, 6H), 2.76–2.84 (m, 2H), 3.93–3.98 (d, J = 14.19 Hz, 1H), 4.11–4.17 (d, J = 14.19 Hz, 1H), 4.19–4.72 (m, 5H), 5.00 (m, 2H), 6.89–7.01 (m, 3H), 7.16–7.24 (m, 5H), 7.63–7.68 (m, 1H), 8.07–8.11 (d, J = 8.91 Hz, 1H), 8.14–8.17 (d, J = 7.59 Hz, 1H), 8.57–8.58 (d, J = 3.96 Hz, 1H), 8.67 (s, 1H), 8.72–8.80 (t, J = 5.6 Hz, 1H), HRFAB-MS: m/z 591.2639 for $[M+H]^+$ (calcd. 591.2641 for $C_{32}H_{39}N_4O_5S$). TOF-MS 591.543 for $[M+H]^+$.

*2,6-Dimethylphenoxyacetyl-Apns-Dmt-NH-4-picolyl (**7h**)*

$[a]_D^{6}$ +36.36 (c = 0.55, CH_3OH), ^1H NMR (DMSO-d_6) δ: 1.37 (s, 3H), 1.55 (s, 3H), 2.12 (s, 6H), 2.71–2.89 (m, 2H), 3.93–3.98 (d, J = 14.19 Hz, 1H), 4.09–4.15 (d, J = 14.19, 1H), 4.32–4.61 (m, 5H), 5.00 (s, 2H), 6.89–7.01 (m, 3H), 7.12–7.26 (m, 5H), 7.63–7.66 (d, J = 5.74 Hz, 2H), 8.09–8.13 (d, J = 9.24 Hz, 1H), 8.58–8.61 (d, J = 6.26 Hz, 2H), 8.77–8.81 (t, J = 5.94 Hz, 1H), HRFAB-MS: m/z 591.2628 for $[M+H]^+$ (calcd. 591.2641 for $C_{32}H_{39}N_4O_5S$).

*2,6-Dimethylphenoxyacetyl-Apns-Dmt-NH-2-picolyl (**7i**)*

$[a]_D^{5}$ +21.80 (c = 0.61, CH_3OH), ^1H NMR (DMSO-d_6) δ: 1.37 (s, 3H), 1.54 (s, 3H), 2.13 (s, 6H), 2.76–2.85 (m, 2H), 3.95–4.00 (d, J = 14.19 Hz, 1H), 4.12–4.17 (d, J = 14.19 Hz, 1H), 4.26–4.56 (m, 5H), 4.94–5.02 (q, J = 9.24 Hz, 2H), 6.89–7.01 (m, 3H), 7.12–7.26 (m, 5H), 7.32–7.37 (t, J = 6.6 Hz, 1H), 7.53–7.56 (d, J = 7.59 Hz, 1H), 7.81–7.87 (t, J = 7.58 Hz, 1H), 8.11–8.14 (d, J = 8.57 Hz, 1H), 8.53–8.54 (d, J = 4.62 Hz, 1H), 8.71–8.75 (t, J = 5.94 Hz, 1H), HRFAB-MS: m/z 591.2631 for $[M+H]^+$ (calcd. 591.2641 for $C_{32}H_{39}N_4O_5S$).

*2,6-Dimethylphenoxyacetyl-Apns-Dmt-NH-(2-hydroxy-4,6-dimethyl)-3-picolyl (**7j**)*

$[a]_D^{6.3}$ −4.28 (c = 0.07, CH_3OH), ^1H NMR (DMSO-d_6) δ: 1.31 (s, 3H), 1.45 (s, 3H), 2.05–2.24 (m, 12H), 2.73–2.80 (m, 2H), 3.98–4.20 (m, 4H), 4.29–4.40 (bs, 1H), 4.44–4.50 (m, 2H), 4.93 (m, 2H), 5.74 (s, 1H), 6.91–7.06 (m, 3H), 7.13–7.37 (m, 5H), 7.98–8.02 (t, J = 5.6 Hz, 1H), 8.13–8.16 (d, J = 7.71 Hz, 1H), HRFAB-MS: m/z 635.2897 for $[M+H]^+$ (calcd. 635.2903 for $C_{34}H_{43}N_4O_6S$).

*2,6-Dimethylphenoxyacetyl-Apns-Dmt-NH-Bz(3-$CONH_2$) (**7k**)*

$[a]_D^{6}$ +42.66 (c = 0.075, CH_3OH), ^1H NMR (DMSO-d_6) δ: 1.34 (s, 3H), 1.51 (s, 3H), 2.14 (s, 6H), 2.71–2.80 (m, 2H), 3.96–4.02 (d, J = 14.19 Hz, 1H), 4.14–4.18 (d, J = 14.19 Hz, 1H), 4.24–4.49 (m, 5H), 4.94–5.03 (m, 2H), 6.90–7.05 (m, 3H), 7.15–7.34 (m, 6H), 7.44–7.48 (d, J = 6.6 Hz, 1H), 7.68–7.70 (d, J = 7.58 Hz, 1H), 7.81 (s, 1H), 7.93 (s, 2H), 8.09–8.13 (d, J = 9.24 Hz, 1H), 8.55–8.62 (t, J = 5.8 Hz, 1H), HRFAB-MS: m/z 633.2756 for $[M+H]^+$ (calcd. 633.2747 for $C_{34}H_{41}N_4O_6S$).

*2,6-Dimethylphenoxyacetyl-Apns-Dmt-NH-Bz(3-$COOCH_3$) (**7l**)*

$[a]_D^{4}$ −13.33 (c = 0.03, CH_3OH), ^1H NMR (DMSO-d_6) δ: 1.33 (s, 3H), 1.51 (s, 3H), 2.13 (s, 6H), 2.75–2.79 (m, 2H), 3.81 (s, 3H), 3.96–4.02 (d, J = 14.19 Hz, 1H), 4.13–4.17 (d, J = 14.19 Hz, 1H), 4.30–4.52 (m, 5H), 4.96–4.98 (m, 2H), 5.50–5.53 (d, J = 8.7 Hz, 1H), 6.92–7.01 (m, 3H), 7.19–7.26 (m, 5H), 7.36–7.42 (t, J = 7.2 Hz, 1H), 7.57–7.61 (d, J = 6.6 Hz, 1H), 7.75–7.78 (d, J = 7.58 Hz, 1H), 7.91 (s, 1H), 8.09–8.12 (d, J = 8.25 Hz, 1H), 8.58–8.62 (t, J = 5.8 Hz, 1H), HRFAB-MS: m/z 648.2753 for $[M+H]^+$ (calcd. 648.2743 for $C_{35}H_{42}N_3O_7S$).

*2,6-Dimethylphenoxyacetyl-Apns-Dmt-NH-Bz(4-$CONH_2$) (**7m**)*

$[a]_D^{5}$ +22.00 (c = 0.05, CH_3OH), ^1H NMR (DMSO-d_6) δ: 1.35 (s, 3H), 1.52 (s, 3H), 2.14 (s, 6H), 2.77–2.89 (m, 2H), 3.96–4.03 (m, 1H), 4.15–4.20 (m, 1H), 4.26–4.52 (m, 5H), 5.00 (s, 2H), 6.90–7.03 (m, 3H), 7.15–7.33 (m, 5H), 7.35–7.40 (d, J = 7.2 Hz, 2H), 7.76–7.81 (d, J = 7.2 Hz, 2H), 7.89 (s, 2H), 8.10–8.15 (d, J = 8.1 Hz, 1H), 8.55–8.60 (t, J = 5.4 Hz, 1H), HRFAB-MS: m/z 633.2763 for $[M+H]^+$ (calcd. 633.2747 for $C_{34}H_{41}N_4O_6S$).

*2,6-Dimethylphenoxyacetyl-Apns-Dmt-NH-Bz(4-$COOCH_3$) (**7n**)*

$[a]_D^{6}$ +16.66 (c = 0.202, CH_3OH), ^1H NMR (DMSO-d_6) δ: 1.35 (s, 3H), 1.52 (s, 3H), 2.14 (s, 6H), 2.76–2.79 (m, 2H), 3.81 (s, 3H), 3.96–4.01 (d, J = 14.19 Hz, 1H), 4.13–4.19 (d, J = 14.51 Hz, 1H), 4.29–4.48 (m, 5H), 4.98 (s, 2H), 6.90–7.01 (m, 3H), 7.18–7.24 (m, 5H), 7.43–7.46 (d, J = 7.26 Hz, 2H), 7.82–7.85 (d, J = 8.24 Hz, 2H), 8.11–8.15 (d, J = 8.75 Hz, 1H), 8.63 (t, J = 5.4 Hz, 1H), HRFAB-MS: m/z 648.2753 for $[M+H]^+$ (calcd. 648.2743 for $C_{35}H_{42}N_3O_7S$).

*Dipeptides containing the 3-hydroxy-2-methylbenzoyl moiety (3-hydroxy-2-methyl benzoyl-Apns-Dmt-P_2') (**8a–h, o, p**)*

To a solution of the appropriate Boc-Apns-Dmt-P_2' **4a–h, o, p** (0.1 mmol) in 4 N HCl/dioxane solution (1 mL), anisole (22 µL, 0.2 mmol) was added at 0°C. The reaction mixture was stirred for 1 h at room temperature. The solvent was removed in vacuum at room temperature; ether was added. After centrifugation, the residue was suspended in AcOEt (5 mL), then Et_3N (17 µL, 0.12 mmol) was added (solution A). 3-Acetyloxy-2-methylbenzoic acid **6** (21.3 mg, 0.11 mmol) was dissolved in AcOEt (5 mL), then Et_3N (17 µL, 0.12 mmol) and DPPCl (25 µL, 0.12 mmol) were added at 0°C. The mixture was stirred at room temperature for 1 h, then mixed with solution A. The mixture was further stirred at room temperature for 6 h, then washed with 10% citric acid, 5% $NaHCO_3$ and brine. The organic layer was dried and evaporated under reduced pressure. The residue was dissolved in methanol (2 mL), then 1 M LiOH (3 mL) was added. Stirring was continued at room temperature for 5 h, followed by addition of 10% citric acid till pH 3. The mixture was extracted with AcOEt and washed with 10% citric acid and brine. The organic extract was dried, evaporated and crystallized from *n*-hexane. The crude product was purified using analytical, preparative and analytical HPLC. The pure product was lyophilized. Physical data are listed in Table 2.

*3-Hydroxy-2-methylbenzoyl-Apns-Dmt-NH-cumyl (**8a**)*

$[a]_D^{3.5}$ +18.69 (c = 0.23, CH_3OH), ^1H NMR (DMSO-d_6) δ: 1.43 (s, 3H), 1.50 (s, 3H), 1.53 (s, 3H), 1.65 (s, 3H), 1.82 (s, 3H), 2.71 (m, 2H), 4.20–4.38 (m, 2H), 4.50–5.51 (d, J = 2.97 Hz,

1H), 4.65 (s,1H), 4.93–4.97 (d, J = 8.9 Hz, 1H), 5.08–5.12 (d, J = 8.9 Hz, 1H), 6.55–6.58 (d, J = 7.26 Hz, 1H), 6.76–6.79 (d, J = 7.91 Hz, 1H), 6.92–7.04 (m, 2H), 7.11–7.19 (m, 7H), 7.40–7.43 (d, J = 8.25 Hz, 2H), 8.19–8.21 (d, J = 8.25 Hz, 1H), 9.22–9.32 (bs, 1H), HRFAB-MS: *m/z* 590.2704 for $[M+H]^+$ (calcd. 590.2689 for $C_{33}H_{40}N_3O_5S$).

3-Hydroxy-2-methylbenzoyl-Apns-Dmt-NH-MPH (8b)

$[\alpha]_D^{26}$ +28.82 (c = 0.17, CH_3OH), ^1H NMR (DMSO-d_6) δ: 1.47 (s, 3H), 1.56 (s, 3H), 1.82 (s, 3H), 2.67–2.87 (m, 2H), 3.06 (s, 3H), 4.41 (s, 2H), 4.49 (s, 1H), 5.02–5.06 (d, J = 8.91 Hz, 1H), 5.14–5.18 (d, J = 9.24 Hz, 1H), 6.54–6.57 (d, J = 7.26 Hz, 1H), 6.66–6.72 (t, J = 7.26 Hz, 1H), 6.76–6.78 (d, J = 7.58 Hz, 1H), 6.87–6.96 (m, 3H), 7.11–7.27 (m, 7H), 8.15–8.19 (d, J = 8.25 Hz, 1H), 9.35 (s, 1H), 10.12 (s,1H), HRFAB-MS: *m/z* 577.2492 for $[M+H]^+$ (calcd. 577.2485 for $C_{31}H_{37}N_4O_5S$).

3-Hydroxy-2-methylbenzoyl-Apns-Dmt-NH-(2-OCH_3)Bz (8c)

$[\alpha]_D^{27.5}$ 0.00 (c = 0.07, CH_3OH), ^1H NMR (DMSO-d_6) δ: 1.35 (s, 3H), 1.51 (s, 3H), 1.84 (s, 3H), 2.69–2.88 (m, 2H), 3.79 (s, 3H), 4.20–4.38 (m, 2H), 4.40–4.48 (m, 3H), 4.99–5.03 (d, J = 9.24, 1H), 5.12–5.16 (d, J = 9.24, 1H), 6.54–6.57 (d, J = 7.26 Hz, 1H), 6.76–6.94 (m, 4H), 7.14–7.33 (m, 7H), 8.12–8.15 (d, J = 8.24 Hz, 1H), 8.25–8.28 (m, 1H), 9.20–9.50 (bs, 1H), HRFAB-MS: *m/z* 592.2472 for $[M+H]^+$ (calcd. 592.2481 for $C_{32}H_{38}N_3O_6S$).

3-Hydroxy-2-methylbenzoyl-Apns-Dmt-NH-(2-OC_2H_5)Bz (8d)

$[\alpha]_D^{25.6}$ +20.32 (c = 0.123, CH_3OH), ^1H NMR (DMSO-d_6) δ: 1.33–1.38 (m, 6H), 1.51 (s ,3H), 1.83 (s, 3H), 2.76–2.88 (m, 2H), 4.00–4.05 (m, 2H), 4.14–4.49 (m, 5H), 5.00–5.03 (d, J = 9.24 Hz, 1H), 5.13–5.16 (d, J = 9.24 Hz, 1H), 6.53–6.56 (d, J = 7.26 Hz, 1H), 6.75–6.84 (m, 2H), 6.91–7.04 (m, 2H), 7.14–7.35 (m, 7H), 8.12–8.15 (d, J = 7.58 Hz, 1H), 8.20–8.30 (m, 1H), 9.35 (s, 1H), HRFAB-MS: *m/z* 606.2652 for $[M+H]^+$ (calcd. 606.2638 for $C_{33}H_{40}N_3O_6S$).

3-Hydroxy-2-methylbenzoyl-Apns-Dmt-NH-Ind (8e)

$[\alpha]_D^{24.2}$ +35.00 (c = 0.22, CH_3OH), ^1H NMR (DMSO-d_6) δ: 1.44 (s, 3H), 1.51 (s, 3H), 1.82 (s, 3H), 2.27–2.49 (m, 2H), 2.75–2.91 (m, 4H), 4.46–4.51 (m, 3H), 5.00–5.04 (m, 1H), 5.06–5.18 (m, 1H), 5.24–5.37 (m, 1H), 6.54–6.57 (d, J = 7.26 Hz, 1H), 6.76–6.79 (d, J = 7.91 Hz, 1H), 6.84–6.95 (m, 1H), 7.10–7.39 (m, 9H), 8.16–8.19 (t, J = 7.59 Hz, 1H), 8.33–8.39 (t, J = 8.91 Hz, 1H), 9.37 (bs, 1H), HRFAB-MS: *m/z* 588.2548 for $[M+H]^+$ (calcd. 588.2532 for $C_{33}H_{38}N_3O_5S$).

3-Hydroxy-2-methylbenzoyl-Apns-Dmt-NH-Pip (8f)

$[\alpha]_D^{24.5}$ +16.36 (c = 0.11, CH_3OH), ^1H NMR (DMSO-d_6) δ: 1.34 (s, 3H), 1.50 (s, 3H), 1.83 (s, 3H), 2.73–2.88 (m, 2H), 4.03–4.10 (m, 1H), 4.28–4.36 (m, 1H), 4.42–4.47 (d, J = 12.7 Hz, 3H), 4.99–5.03 (d, J = 9.24 Hz, 1H), 5.12–5.16 (d, J = 8.9 Hz, 1H), 5.90–5.96 (m, 2H), 6.54–6.57 (d, J = 7.26 Hz, 1H), 6.73–6.88 (m, 4H), 6.92–6.98 (t, J = 7.92 Hz, 1H), 7.16–7.33 (m, 5H), 8.11–8.14 (d, J = 7.92 Hz, 1H), 8.37–8.39 (t, J = 5.61 Hz, 1H), 9.20–9.60 (bs, 1H), HRFAB-MS: *m/z* 606.2269 for $[M+H]^+$ (calcd. 606.2274 for $C_{32}H_{36}N_3O_7S$).

3-Hydroxy-2-methylbenzoyl-Apns-Dmt-NH-3-picolyl (8g)

$[\alpha]_D^{25.8}$ +15.62 (c = 0.224, CH_3OH), ^1H NMR (DMSO-d_6) δ: 1.32 (s, 3H), 1.50 (s, 3H), 1.82 (s, 3H), 2.68–2.86 (m, 2H), 4.15–4.23 (m, 1H), 4.28–4.47 (m, 4H), 5.00–5.03 (d, J = 8.91, 1H), 5.13–5.17 (d, J = 9.23 Hz, 1H), 5.49–5.52 (d, J = 6.6 Hz, 1H), 6.53–6.56 (d, J = 7.26 Hz, 1H), 6.76–6.79 (d, J = 7.91 Hz, 1H), 6.90–6.98 (m, 1H), 7.13–7.31 (m, 6H), 7.67–7.70 (d, J = 7.58 Hz, 1H), 8.12–8.15 (d, J = 7.91 Hz, 1H), 8.39–8.53 (m, 3H), 9.38 (bs, 1H), HRFAB-MS: *m/z* 563.2341 for $[M+H]^+$ (calcd. 563.2328 for $C_{30}H_{35}N_4O_5S$).

3-Hydroxy-2-methylbenzoyl-Apns-Dmt-NH-4-picolyl (8h)

$[\alpha]_D^{27.5}$ +25.92 (c = 0.135, CH_3OH), ^1H NMR (DMSO-d_6) δ: 1.37 (s, 3H), 1.55 (s, 3H), 1.80 (s, 3H), 2.70–2.90 (m, 2H), 4.20–4.66 (m, 5H), 5.01–5.05 (d, J = 8.7 Hz, 1H), 5.15–5.19 (d, J = 8.9 Hz, 1H), 6.53–6.55 (d, J = 7.26 Hz, 1H), 6.73–6.76 (d, J = 7.9 Hz,1H), 6.86–6.92 (t, J = 7.83 Hz 1H), 7.05–7.32 (m, 4H), 7.66–7.68 (d, J = 5.74 Hz, 2H), 8.08–8.12 (d, J = 7.9 Hz, 1H), 8.26 (d, J = 1.7 Hz 1H), 8.56–8.60 (d, J = 6.26 Hz, 2H), 8.70–8.76 (m, 1H), 9.35–9.45 (bs, 1H), HRFAB-MS: *m/z* 563.2337 for $[M+H]^+$ (calcd. 563.2328 for $C_{30}H_{35}N_4O_5S$).

3-Hydroxy-2-methylbenzoyl-Apns-Dmt-NH-1-Adam (8o)

$[\alpha]_D^{18.5}$ +7.45 (c = 0.295, CH_3OH), ^1H NMR (DMSO-d_6) δ: 1.41 (s, 3H), 1.48 (s, 3H), 1.61 (s, 6H), 1.82–1.96 (m, 12H), 2.69–2.82 (m, 2H), 4.24–4.42 (m, 1H), 4.53 (s, 2H), 4.94–4.97 (d, J = 9.23 Hz, 1H), 5.15–5.18 (d, J = 8.25 Hz, 1H), 6.55–6.57 (d, J = 6.93 Hz, 1H), 6.76–6.79 (d, J = 7.58 Hz, 1H), 6.91–6.94 (m, 1H), 7.07–7.23 (m, 3H), 7.37–7.39 (d, J = 6.92 Hz, 2H), 7.49 (s, 1H), 8.22–8.25 (d, J = 8.25 Hz, 1H), 9.20–9.60 (bs, 1H), HRFAB-MS: *m/z* 606.3011 for $[M+H]^+$ (calcd. 606.3002 for $C_{34}H_{44}N_3O_5S$).

3-Hydroxy-2-methylbenzoyl-Apns-Dmt-NH-2-Adam (8p)

$[\alpha]_D^{20}$ +11.81 (c = 0.127, CH_3OH), ^1H NMR (DMSO-d_6) δ: 1.38 (s, 3H), 1.48–1.52 (m, 6H), 1.69–2.09 (m, 15H), 2.65–2.81 (m, 2H), 3.89 (s, 1H), 4.31–4.37 (m, 1H), 4.51 (s, 1H), 4.70 (s, 1H), 4.99–5.02 (d, J = 8.91 Hz, 1H), 5.13–5.16 (d, J = 8.58 Hz, 1H), 6.53–6.56 (d, J = 7.59 Hz, 1H), 6.76–6.78 (d, J = 7.25 Hz, 4H), 6.91–6.93 (t, J = 7.58 Hz, 1H), 7.08–7.32 (m, 5H), 7.81–7.84 (d, J = 6.26 Hz, 1H), 8.19–8.22 (d, J = 7.92 Hz, 1H), HRFAB-MS: *m/z* 606.3011 for $[M+H]^+$ (calcd. 606.3002 for $C_{34}H_{44}N_3O_5S$).

HIV protease inhibition

HIV protease inhibition was determined by an HPLC method using S10 peptide (H-Lys-Ala-Arg-Val-Tyr*Phe(p-NO_2)-Glu-Ala-Nle-NH_2) as the enzyme substrate. The inhibitory potentials were tested at 50 nM concentration of the inhibitor. The assay protocol was followed as described by Mimoto et al. [15].

References

[1] A.Carrillo, K. D. Stewart, H. L. Sham, D. W. Norbeck, W. E. Kohlbrenner, J. M. Leonard, D. J. Kempf, A. Monna, *J. Virol.* **1998**, *72*, 7532–7541.

[2] L. Tong, S. Pav, S. Mui, D. Lamarre, C. Yoakim, P. Beaulieu, P. C. Anderson, *Structure* **1995**, *3*, 33–40.

[3] A. A. Bekhit, H. Matsumoto, H. M. M. Abdel-Rahman, T. Mimoto, S. Nojima, H. Takaku, T. Kimura, K. Akaji,

Y. Kiso; "Peptide Science – Present and Future", Proceedings of the 1st International Peptide Symposium, Ed. Y. Shimonishi, Kluwer Academic Publishers, Dordrecht, 1999, pp. 660–661.

[4] R. S. Randad, L. Lubkowska, T. N. Bhat, S. Munshi, S. V. Gulnik, B. Yu, J. W. Erickson, *Bioorg. Med. Chem. Lett.* **1995**, *5*, 1707–1712.

[5] R. S. Randad, L. Lubkowska, A. M. Silva, D. M. A. Guerin, S. V. Gulnik, B. Yu, J. W. Erickson, *Bioorg. Med. Chem.* **1996**, *4*, 1471–1480.

[6] D. J. Kempf, C. A. Flentge, N. E. Wideburg, A. Saldivar, S. Vasavanonda, D. W. Norbeck, *Bioorg. Med. Chem. Lett.* **1995**, *5*, 2725–2728.

[7] Y. Kiso, S.Yamaguchi, H. Matsumoto, T. Mimoto, R. Kato, S. Nojime, H. Takaku, T. Fukkazawa, T. Kimura, K. Akaji, *Arch. Pharm. Pharm. Med. Chem.* **1998**, *331*, 87.

[8] M. S. Roger, H. B. Christina, *J. Chromatogr.* **1989**, *475*, 57.

[9] P. Ruelle, W. K. Ulrich, *J. Pharm. Sci.* **1998**, *87*, 987.

[10] M.Schutkowski, C. Mrestani-Klaus, K. Neubert, *Int. J. Peptide Protein Res.* **1995**, *45*, 257–265.

[11] D.Hudson, *J. Org. Chem.* **1988**, *53*, 617–624.

[12] T. Miyazawa, T. Yamada, S. Kuwata, *Bull. Chem. Soc. Jpn.* **1988**, *61*, 606–608.

[13] A. S. Kende, D. Scholz, J. Schneider, *Synth. Commun.* **1978**, *8*, 59–63.

[14] J. Dudash, Jr., J. Jiang, S. C. Mayer, M. M Joullie, *Synth. Commun.* **1993**, *23*, 349–356.

[15] T. Mimoto, R. Kato, H. Takaku, S. Nojima, K. Terashima, S. Misawa, T. Fukazawa, T. Ueno, H.Sato, M. Shintani, Y. Kiso, H. Hayashi, *J. Med. Chem.* **1999**, *42*, 1789–1802.

[16] H. M. M. Abdel-Rahman, Ph.D. Thesis, Assiut University, Egypt, **1999**.

[17] Y. Kiso, *Biopolymers (Peptide Science)* **1996**, *40*, 235–244.

[18] M. M. Sheha, N. M. Mahfouz, H. Y. Hassan, A. F. Youssef, T. Mimoto, Y. Kiso, *Eur. J. Med. Chem.* **2000**, *35*, 887–894.

Available online at www.sciencedirect.com
SCIENCE DIRECT®
Bioorganic & Medicinal Chemistry Letters
ELSEVIER
Bioorganic & Medicinal Chemistry Letters 15 (2005) 211–215

Design and synthesis of highly active Alzheimer's β-secretase (BACE1) inhibitors, KMI-420 and KMI-429, with enhanced chemical stability

Tooru Kimura,[a,b] Daisuke Shuto,[a] Yoshio Hamada,[a,b] Naoto Igawa,[a] Soko Kasai,[a] Ping Liu,[a] Koushi Hidaka,[a,b] Takashi Hamada,[a] Yoshio Hayashi[a,b] and Yoshiaki Kiso[a,b,*]

[a]*Department of Medicinal Chemistry, Center for Frontier Research in Medicinal Science, Kyoto Pharmaceutical University, Yamashina-ku, Kyoto 607-8412, Japan*
[b]*21st Century COE Program, Kyoto Pharmaceutical University, Yamashina-ku, Kyoto 607-8412, Japan*

Received 30 August 2004; accepted 30 September 2004
Available online 22 October 2004

Abstract—Recently, we reported potent and small-sized BACE1 inhibitors KMI-358 and KMI-370 in which the Glu residue is replaced by a β-*N*-oxalyl-DAP (L-α,β-diaminopropionyl) residue at the P_4 position. The β-*N*-oxalyl-DAP group is important for enhancing BACE1 inhibitory activity, but these inhibitors isomerized to α-*N*-oxalyl-DAP derivatives in solvents. Hence, we used a tetrazole moiety as a bioisostere of the free carboxylic acid of the oxalyl group. KMI-420 and KMI-429, containing a tetrazole ring, showed improved stability and potent enzyme inhibitory activity.

1. Introduction

Amyloid β peptide (Aβ), which is the main component of senile plaques found in the brains of Alzheimer's disease (AD) patients,[1] is formed by proteolytic processing of amyloid precursor protein (APP).[2,3] Since BACE1 (β-site APP cleaving enzyme, β-secretase) triggers Aβ formation by cleaving at the *N*-terminus of the Aβ domain,[4–7] it is a molecular target for therapeutic intervention in AD.[8–11] Recently, we reported on the BACE1 inhibitors, KMI-300 (**1b**), -358 (**2b**), and -370 (**3b**)[12] (Fig. 1), which contained phenylnorstatine [Pns: (2*R*,3*S*)-3-amino-2-hydroxy-4-phenylbutyric acid] as a substrate transition-state mimic.[13,14] These inhibitors were designed from the octapeptide BACE1 inhibitor KMI-008[11] as the lead compound. However, inhibitors, **1b–3b**, have labile β-*N*-oxalyl-DAP residues (DAP: L-α,β-diaminopropionic acid) at the P_4 position. β-*N*-oxalyl-DAP is known as the neurotoxic constituent of the legume *Lathyrus sativus*,[15–17] which thermally isomerizes to an equilibrium mixture with α-*N*-oxalyl-DAP.[18,19] Similarly, the compounds **1b–3b** are converted to α-*N*-oxalyl-DAP derivatives (Fig. 2), which show the low enzyme inhibitory activities, in aqueous and organic

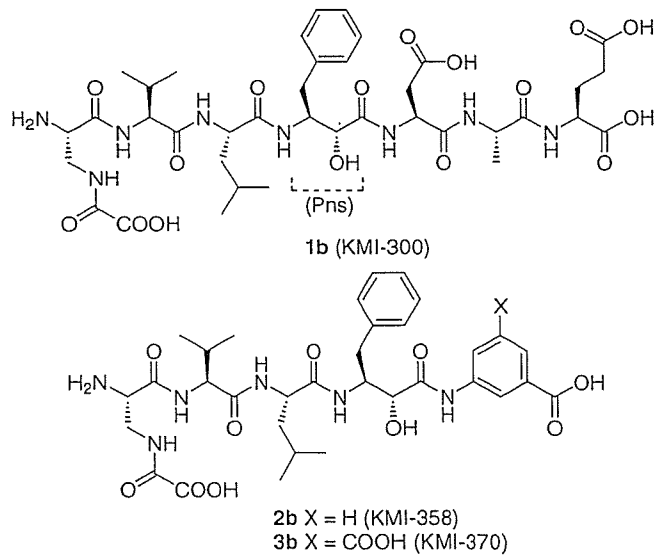

Figure 1. Structure of BACE1 inhibitors containing β-oxalyl-DAP residue at the P_4 position.

Keywords: Alzheimer's disease; BACE1 inhibitor; β-Secretase; Bioisostere.
* Corresponding author. Tel.: +81 75 595 4635; fax: +81 75 591 9900; e-mail: kiso@mb.kyoto-phu.ac.jp

0960-894X/$ - see front matter © 2004 Elsevier Ltd. All rights reserved.
doi:10.1016/j.bmcl.2004.09.090

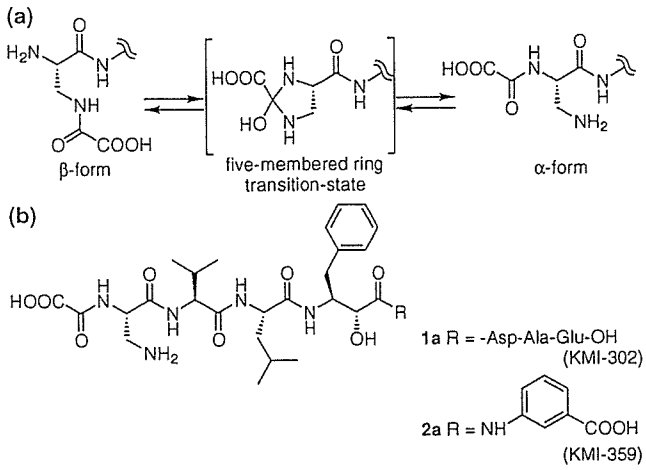

Figure 2. (a) Isomerization of oxalyl-DAP derivatives. (b) Structure of BACE1 inhibitor's isomers containing α-oxalyl-DAP residue at the P_4 position.

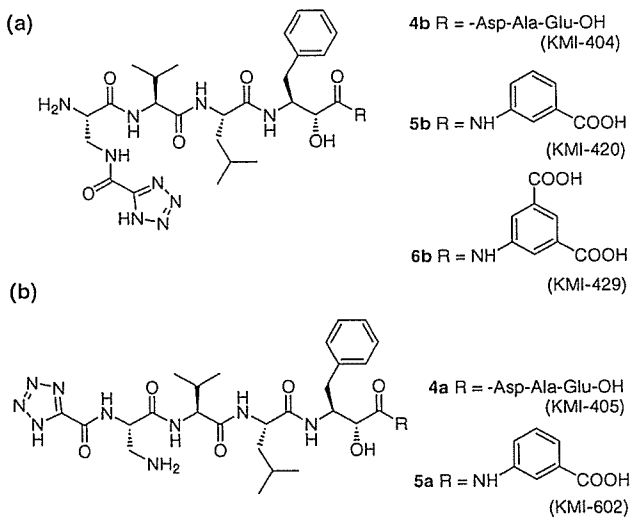

Figure 3. Structure of BACE1 inhibitors containing a tetrazole ring at the P_4 position (a) and their α-isomers (b).

solvents. To improve the stability of compounds **1b–3b**, the oxalyl moiety was replaced with tetrazole carbonyl derivatives as a bioisostere[20] of carboxylic acid. Consequently, we found the tetrazole-containing BACE1 inhibitors **4b–6b** (Fig. 3), with enhanced chemical stability and enzyme inhibitory activity.

2. Synthesis

BACE1 inhibitors (**4b** and **5b**) and α-isomers (**1a**, **2a**, **4a**, and **5a**) were synthesized by the 9-fluorenylmethoxycarbonyl (Fmoc)-based solid phase peptide synthesis as previously reported.[12] As an example, Scheme 1 shows the synthesis of **5b** (KMI-420). Namely, the *N*-Fmoc-3-aminobenzoic acid was attached to 2-chlorotrityl chloride resin using diisopropylethylamine (DIPEA) in dichloromethane (DCM). The Fmoc group was removed with 20% piperidine in DMF and the peptide

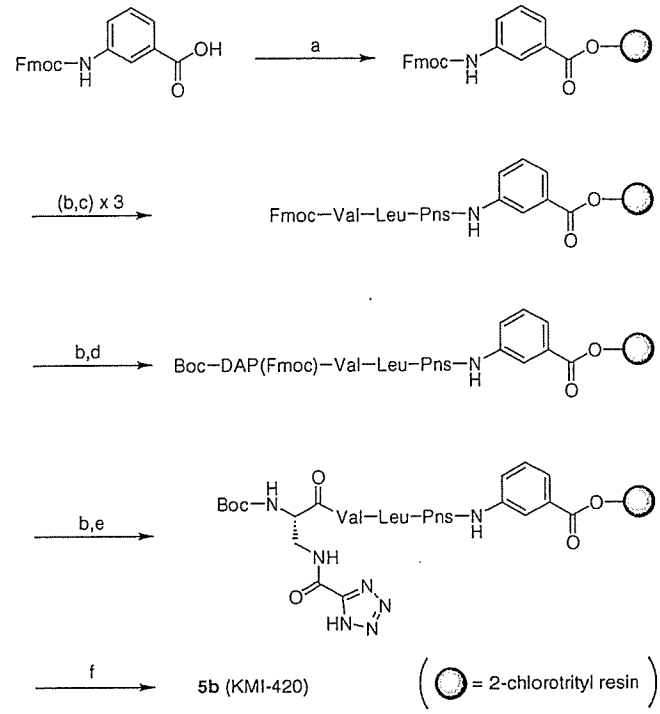

Scheme 1. Reagents and conditions: (a) 2-chlorotrityl chloride resin, DIPEA/DCM; (b) 20% piperidine/DMF; (c) Fmoc-AA-OH, DIPCDI, HOBt/DMF; (d) Boc-DAP(Fmoc)-OH, DIPCDI, HOBt/DMF; (e) 1*H*-tetrazole-5-carboxylic acid, DIPCDI, HOBt/DMF; (f) TFA, *m*-cresol, thioanisole.

bonds were formed using diisopropylcarbodiimide (DIPCDI) in the presence of 1-hydroxybenzotriazole (HOBt). The coupling of Boc-Pns-OH and aminobenzoyl resin was achieved using the same manner reported previously[12] without any problem. The DAP residue at the P_4 position was introduced using N^{α}-Boc-N^{β}-Fmoc-L-2,3-diaminopropionic acid [Boc-DAP-(Fmoc)-OH]. The β-substituted DAP moiety in **4b** (KMI-404) was introduced in a manner similar to that in **5b**. However, for the α-substituted derivatives (**1a**, **2a**, **4a** and **5a**), the DAP residue at the P_4 position was introduced using N^{β}-Boc-N^{α}-Fmoc-L-2,3-diaminopropionic acid [Fmoc-DAP(Boc)-OH]. After peptide chain elongation, the 1*H*-tetrazole-5-carbonyl residue at the β-position of DAP was introduced using 1*H*-tetrazole-5-carboxylic acid. Finally, the peptide was cleaved from the resin by treatment with trifluoroacetic acid (TFA) in the presence of *m*-cresol and thioanisole. The crude peptide was purified by preparative RP-HPLC. On the other hand, the α-oxalyl residue at the P_4 position in compounds **1a** and **2a** was introduced using oxalic acid mono-*t*-butyl ester.

Compound **6b** (KMI-429), which contained 5-aminoisophthalic acid at the C-terminus, was synthesized by a traditional solution method (Scheme 2). Dibenzyl 5-aminoisophthalate was used as a starting compound and 1-ethyl-3-(3-dimethylaminopropyl)carbodiimide·HCl (EDC·HCl) in the presence of HOBt formed the peptide bonds. Boc and Fmoc groups were deprotected using 4 M HCl in dioxane and 20% diethylamine in DMF,